Polymer Electrets for Organic Nonvolatile Memory Devices: Recent Advances

Yi Jie Eng,[a] Yi-Hsun Weng,[b] Algin Biying Oh,[a] Cheng-Liang Liu,[c] Julian M. W. Chan*[a]

[a] Institute of Sustainability for Chemicals, Energy and Environment ($ISCE^2$),

Agency for Science, Technology and Research (A*STAR),

1 Pesek Road, Jurong Island, Singapore 627833,

Republic of Singapore

*E-mail: julian_chan@isce2.a-star.edu.sg

[b] Department of Chemical Engineering,

National Taiwan University,

Taipei 10617, Taiwan

[c] Department of Materials Science and Engineering and Advanced Research Center

for Green Materials Science and Technology,

National Taiwan University,

Taipei 10617, Taiwan

ABSTRACT

Compared to conventional electronics, organic electronics enjoy advantages such as mechanical flexibility, amenability to low-cost processing, and facile tunability of optoelectronic properties via rational molecular design. Within organic electronics, organic (photo)memory has emerged as a sub-area of considerable interest over the last decade. Besides the organic semiconductor, the other critical component of organic transistor-based memory devices is the polymer electret. Polymer electrets form the charge-trapping dielectric layer that is key to the function of memory devices. Like semiconductors, polymer electrets can also be rationally tailored at the molecular level to render optimal properties. To date, there have been many intriguing classes of polymers developed for memory applications. In this review, we present notable recent advances featuring structurally diverse polymer electrets in organic (photo)memory devices. Four categories of polymers will be discussed: (1) pendent sidechain polymers, (2) π-conjugated polymers, (3) block copolymers, and (4) other polymeric systems.

1. Introduction

Many innovations in optoelectronic technologies have been developed based on memory transistor frameworks, examples of which include high-density data storage, [1,2] photorecorders, [3] pattern/image identification, [4,5] ultrasensitive photodetectors, [6] artificial synapses, [7,8] and pulse monitoring sensors. [9] In the wake of the rapid growth of the Internet of Things (IoT), machine learning (ML), and artificial intelligence (AI), it has become increasingly essential to develop ever-higher computing power and larger data storage capabilities. Traditional memory based on optical, electronic, and magnetic technologies come with their own advantages and limitations. For example, dynamic random-access memory (DRAM) supports fast reading and writing but requires high power consumption to refresh the memory unit. On the other hand, flash memory technologies possess longer retention times than DRAM, but suffer from slower programming/erasing speeds. [10] Hence, emerging memory storage technologies have pivoted on the use of various advanced materials to circumvent these aforementioned shortcomings. Nonvolatile memory devices are a type of data storage technology that retain stored information even when the power supply is turned off. With the increasing demand for lightweight and flexible nonvolatile memory electronics for specialized applications, organic field-effect transistors (OFETs) have gained much attention in the research community due to their inherent flexibility, light weight, and potential for facile low-cost, large-area processing and fabrication. [11, 12] Another unique benefit offered by organic memory devices is the tunability afforded by the organic components, e.g., the polymer electret and the organic semiconductor, whose structures can be readily and rationally modified and fine-tuned at the molecular level via organic synthesis. The same level of control is not achievable with inorganic materials. In regard to applications, organic memory devices offer advantages such as their nondestructive readouts, multibit data storage, readily integrated structures, and high compatibility with complementary oxide semiconductors (CMOS) for

integrated circuit design. Their intrinsic light-weight and flexible nature make them ideally suited for fabricating affordable next-generation wearable devices. In today's information-driven world, rapid data generation can exceed storage capacity in digital technologies. Delays arising from the continuous data exchange between processors and memory devices can limit computing speed and energy efficiency, i.e., the von Neumann bottleneck. It has thus become imperative to develop next-generation nonvolatile memory technologies that can accommodate simultaneous data processing and information storage. To that end, OFET memories have also garnered much attention due to their potential for multibit data storage, photoprogramming, low energy consumption, and broad response to different optical bands.

In terms of their architecture, OFET-based memory devices feature at least one additional polarization/charge storage electret layer between the organic semiconductor and the gate contact. This charge-trapping layer allows for the modulation of electrical behavior and thus represents a tunable component that could promote more pronounced hysteresis and/or threshold voltage shifts needed for enhanced memory performance. [13] Generally, OFET memories may be categorized based on the class of charge-storage materials employed: (1) floating-gate, (2) ferroelectric, (3) polymer electret. Polymer electrets are a class of dielectric materials (i.e., polymeric organic insulators) that are capable of trapping electrostatic charges to set up a transient electric field and/or dipole moment. The trapping of charges within polymer electrets may be rooted in one or more of the following mechanisms: (i) presence of structural defects as well as impurity centers; (ii) accumulation of charges proximal to heterogeneities, e.g., grain boundaries in polycrystalline materials or crystalline-amorphous interfaces in semicrystalline polymers, and (iii) orientation of dipoles in polar materials. [14] In terms of structure-property relationships, non-polar or hydrophobic polymers are generally more effective as polymer electrets compared to polar hydrophilic ones that may facilitate charge dissipation via conductive pathways that could form from dipoles, ions, and moisture. [14]

Polymer electret-based transistor memory devices have also been shown to have faster writing and erasing speeds, higher on/off current ratios, larger memory windows, and greater stability compared with ferroelectric or floating-gate transistor memories. [15] Consequently, the design and synthesis of novel polymer electret systems for superior memory performance continues to be a highly active area of research.

In this review, we first present a brief treatment of the operating principles behind OFET-based memory devices, followed by an in-depth survey of notable recent advances in the field of polymer electret-based OFET memory devices. Discussion will be categorized by the class of polymer electret, namely: (1) pendent sidechain polymers, (2) π-conjugated polymers, (3) block copolymers, and (4) other polymer systems, i.e., structures that do not fall under the preceding categories, including unusual and recently reported biomass-derived polymer systems. Herein, we discuss the characteristic chemical structures and synthesis of a diverse range of polymers, highlight key properties, and compare device performance results between the different types of electrets used in nonvolatile OFET memory applications in the recent years (i.e., past 4 years). Lastly, we conclude by discussing the future outlook of polymer electret development for next-generation organic nonvolatile memory devices.

2. Operating principle of OFET memory devices

The conventional architecture of an organic transistor-based memory device is composed of three terminals (source, drain, and gate) plus a polymer electret layer sandwiched between the organic semiconductor and dielectric layers (Fig. 1(a)). In the case of a *p*-type OFET, applying a sufficiently high negative gate voltage (V_g) would cause holes to accumulate at the bottom of the semiconductor interface to form a conductive accumulation region. A negative voltage difference (V_{ds}) between the drain and source drives the hole current in the accumulation region, creating the output drain current (I_d). [16] Hence, an OFET can be characterized by its transfer characteristic curve (I_d against V_g) and output characteristic curve

(I_d against V_{ds}). The slope of the $I_d^{½}$–V_g plot is linearly proportional to the field-effect charge carrier mobility (μ), while threshold voltage (V_{th}) is the minimum V_g needed to create a conducting channel between the source and drain and this can be determined from the extrapolating the curve $I_d^{½}$ vs. V_g to $I_d = 0$. The programming or erasing operation of the memory device is hence facilitated by charge localization in the polymer electret layer through the application of a V_g bias to vary the carrier distribution within the semiconducting channel (Fig. 1(b)). Several parameters can be used to define OFET-based memory characteristics, including its memory window, memory ratio, retention, and endurance. The memory window indicates the information storage level, which is defined by the shift in V_{th} during different operations ($\Delta V_{th} = \Delta N \times e/C_i$), where ΔN is the number of trapped charge carriers in the electret, e is the elementary charge, and C_i is the total capacitance of the electret and the blocking dielectric. A large shift in V_{th} would signify a larger memory window and higher memory ratio. Memory ratio is defined as the I_d difference between the programmed and erased states at a fixed read voltage (V_{read}). Memory retention measures the ability of the memory device to preserve its programmed and erased states without losing the localized charges via leakage paths over time and this is generally on the order of 10^3 to 10^6 s (Fig. 1(c)). [17] Finally, the cycling endurance of a memory device refers to the write-read-erase-read (WRER) cycles that is used to evaluate the reliability and stability of the device (Fig. 1(d)), [18,19] values of which are typically in the range of 10^2 to 10^5 cycles. Table 1 summarizes the selected polymer electrets featured in this review, gate dielectrics, device operations, and their memory performance.

Table 1. Featured organic nonvolatile memory devices and their characteristics.

Channel	Electret	Dielectric (thickness)	Operations[a]	Light [mW cm^{-2}][b]	Mobility [cm^2 V^{-1} s^{-1}][c]	ΔV_{th} [V][d]	Retention test[e]	WRER stability[f]	Ref.
C12-BTBT	PFS	SiO_2 (300 nm)	EP: V_g = 100 V; EE: V_g = -100 V	NA	11.2	108	10^7; 10^4 s	NA	[27]
pentacene	TTC/C_{60}	CP2 (>100 nm)	EP: V_g = 20 V; EE: V_g = -20 V	NA	NA	~7	> 10^2; 2 × 10^4 s	> 10^2; 200 cycles	[28]
DNTT	PVPh:TCPP	SiO_2 (100 nm)	PW: V_d = -40 V; EE: V_g = -30 V	20; 450 nm	0.235	18.2	1.12 × 10^8; 10^4 s	> 10^5; 10 cycles	[29]
pentacene	PVK (Mw = 1.1× 10^6)	SiO_2 (50 nm)	PEP: V_d = -15 V, V_g = 10 V; EE: V_g = -30 V	18.8; white	0.10	15.8	> 10^1; 2 × 10^4 s	> 10^2; 200 cycles	[30]
pentacene	copoly(CBT)	SiO_2 (300 nm)	PW: V_d = -60 V; EE: V_g = -90 V	25; white	NA	49	10^3; 10^4 s	> 10^2; 50 cycles	[44]
pentacene	Shell: PEGMA Core: PV2T-BT	SiO_2 (100 nm)	PW: V_d = -40 V; EE: V_g = -60 V	10; 405 nm	1.1 × 10^{-3}	17.0	10^6; 10^4 s	> 10^4; 10 cycles	[45]
pentacene	PTPA-CNBr	SiO_2 (300 nm)	PW: V_d = -60 V; EE: V_g = -50 V	NA; blue	NA	NA	> 10^5; 400 s	NA	[47]
pentacene	PFO_{5k}-*b*-PS_{22k}	SiO_2 (100 nm)	PEP: V_d = -60 V, V_g = -10 V; EE: V_g = -40 V	30; 405 nm	7.4 × 10^{-3}	21	10^4; 10^4 s	5 × 10^3; 10 cycles	[48]
PTCDI-C8	PF-*b*-PDL_3	SiO_2 (300 nm)	EP: V_g = -140 V; EE: V_g = 140 V	NA	1.06 × 10^{-3}	102	> 10^4; 10^4 s	> 10^3; 16 cycles	[49]
pentacene	PF-*b*-$Piso_{20}$	SiO_2 (100 nm)	PW: V_d = -40 V; EE: V_g = -40 V	30; 405 nm	0.025	33	10^6; 10^4 s	10^4; 10 cycles	[50]
C8-BTBT	PF-*b*-PNIPAAms (7-188)	SiO_2 (100 nm)	PW: V_d = -15 V; EE: V_g = -30 V	2; 365 nm	0.025	23.12	> 10^5; 10^3 s	> 10^5; 11 cycles	[51]
pentacene	PEO_{5k}-*b*-$PPyMA_{10.2k}$(SA)	SiO_2 (100 nm)	PW: V_d = -40 V; EE: V_g = -50 V	5; 405 nm	4.6 × 10^{-4}	54	> 10^6; 10^4 s	10^5; 100 cycles	[53]

pentacene	P2	PI(ISBA-BPDA) (238 nm)	PW: V_d = -60 V; EE: V_g = -60 V	0.95; 365 nm	0.015	NA	1.3×10^3; 10^4 s	2.9×10^2; 50 cycles	[54]
pentacene	PPIX/PLA (1/2)	PI(ISBA-BPDA) (302 nm)	PW: V_d = -60 V; EE: V_g = -60 V	0.95; 405 nm	8.2×10^{-3}	NA	8.9×10^5; 10^4 s	NA	[55]
pentacene	PI-SM5	SiO_2 (300 nm)	PEP: V_d = -100 V, V_g = 100 V; EE: V_g = -100 V	0.72; 365 nm	NA	37.2	$> 10^4$; 10^4 s	$> 10^4$; 10 cycles	[58]
pentacene	CNBr-PES	SiO_2 (100 nm)	PW: V_d = -5 V; EE: V_g = -10 V	5; 365 nm	0.05	50	$> 10^5$; 10^3 s	$> 10^3$; 500 cycles	[59]

[a] The device encrypting operations. EE: electrical writing; EP: electrical programming; PW: photowriting; PEP: photoassisted electrical programming. [b] The irradiance and the wavelength of light. [c] Carrier mobility of the transistor memories. [d] ΔV_{th}: memory window. [e] The memory ratio after retention test. [f] The memory ratio after WRER cycles.

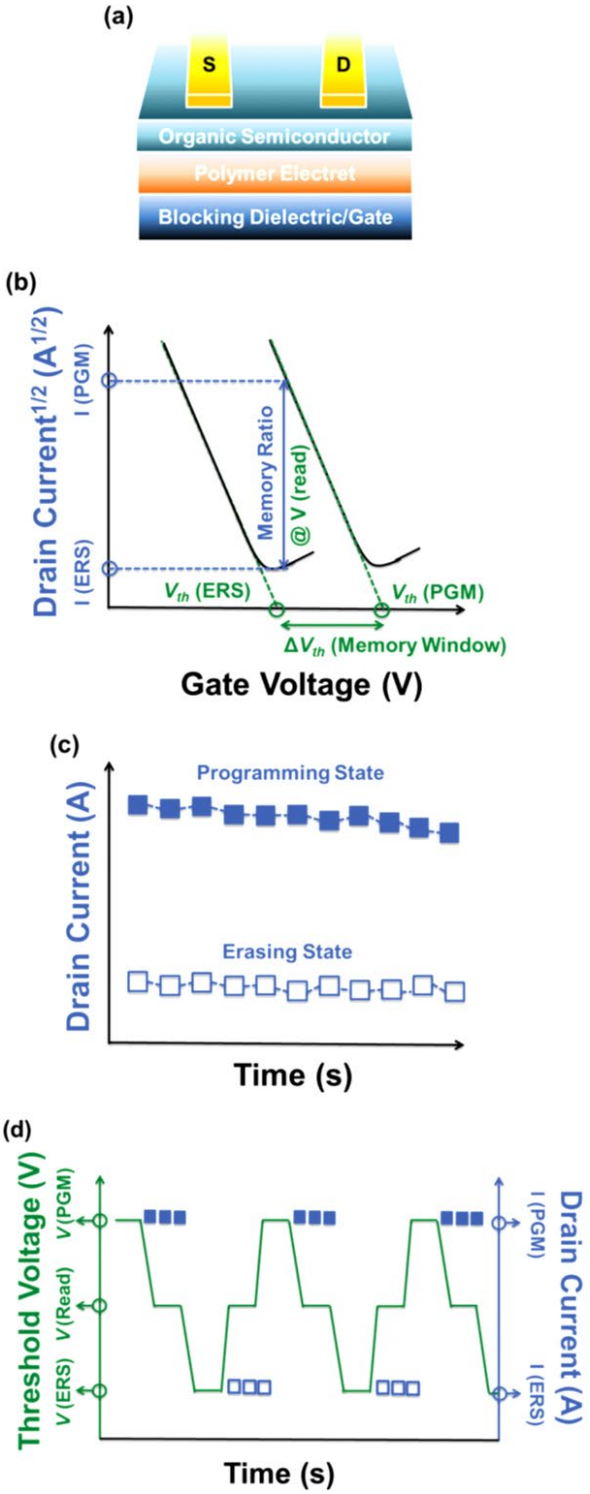

Fig. 1. (a) Schematic configuration of an OFET memory device. (b) $I_d^{1/2}$ vs. V_g curve under applied voltage bias that determines the memory window and memory ratio. (c) Retention time and (d) Endurance cycles of OFET-based memory devices. Reprinted from ref. [19] with permission from The Royal Society of Chemistry.

The electrical/optical operations and corresponding charge distributions of a *p*-type transistor memory device are depicted in Fig. 2. Regarding a transistor memory designed for all electrical operation, a negative gate bias is applied for electrical erasing. This leads to the tunneling of holes within the organic semiconductor (OSC) channel into the HOMO of the polymer electret. The transfer curve of the electrically erased state is negatively shifted due to the screening effect of the gate voltage induced by the trapped hole carriers (Fig. 2(a)). [20] Subsequently, a positive gate bias is applied for electrical programming. This operation results in the back-tunneling of the trapped holes and the injection of electrons from the source/drain electrode. Driven by coulombic interactions between the oppositely charged species, the free electrons/holes would then undergo exciton recombination in the OSC or polymer electret. In the electrically programmed state, the transfer curve will revert to its initial state or to an even more positive state as determined by the number of trapped electrons (Fig. 2(b)). On the other hand, photowriting may be utilized as an alternative to electrical programming in a photomemory device. During the photowriting process, external photoexcitation is carried out under a negative drain voltage and zero gate voltage. This generates an exciton, which then diffuses to the OSC/electret interface and dissociates into free carriers if the photon energy exceeds the exciton binding energy. The newly generated hole carriers drift toward the HOMO of the OSC to yield an enhanced photocurrent, while electrons recombine with the original trapped holes. The transfer curve of the photowritten state is also positively shifted due to the recombined holes or newly trapped electrons (Fig. 2(c)). Photoassisted electrical programming is a combined operation comprising electrical programming and photowriting. This operation utilizes both gate voltage and photoexcitation at the same time, and it can generate a more profound shift of the transfer curve. The major difference between an electrically programmed state and a photowritten state in the way the charge carriers are trapped. Additionally, the evaluation of the subthreshold swing (SS) provides insight into the trapping mechanism. [21]

SS is the inverse slope of the transistor's transfer characteristics in the subthreshold region and is defined as the gate voltage required to increase the drain current by one order of magnitude. The equation $SS = (k_BT \times \ln 10/e) \times (N_t \times e^2/C_i + 1)$ reflects the relationship of SS and the charge trapping type, where k_B is the Boltzmann constant, T is the absolute temperature, and N_t is the interfacial trapped charges in the OSC. [22] The transfer curve of the photowritten state shows a larger SS in the subthreshold region, while the SS of the electrically programmed state remains nearly unchanged. The larger SS in the former case is due to photogenerated holes from the polymer electret filling up shallow traps in the HOMO of the OSC. These shallow traps originate from the disorder at the semiconductor interface, which give rise to trapping sites above the hole transport edge. In the case of electrical programming, the injected electron carriers maintain a balanced carrier concentration in the OSC, thereby resulting in parallel shifting of the transfer curves.

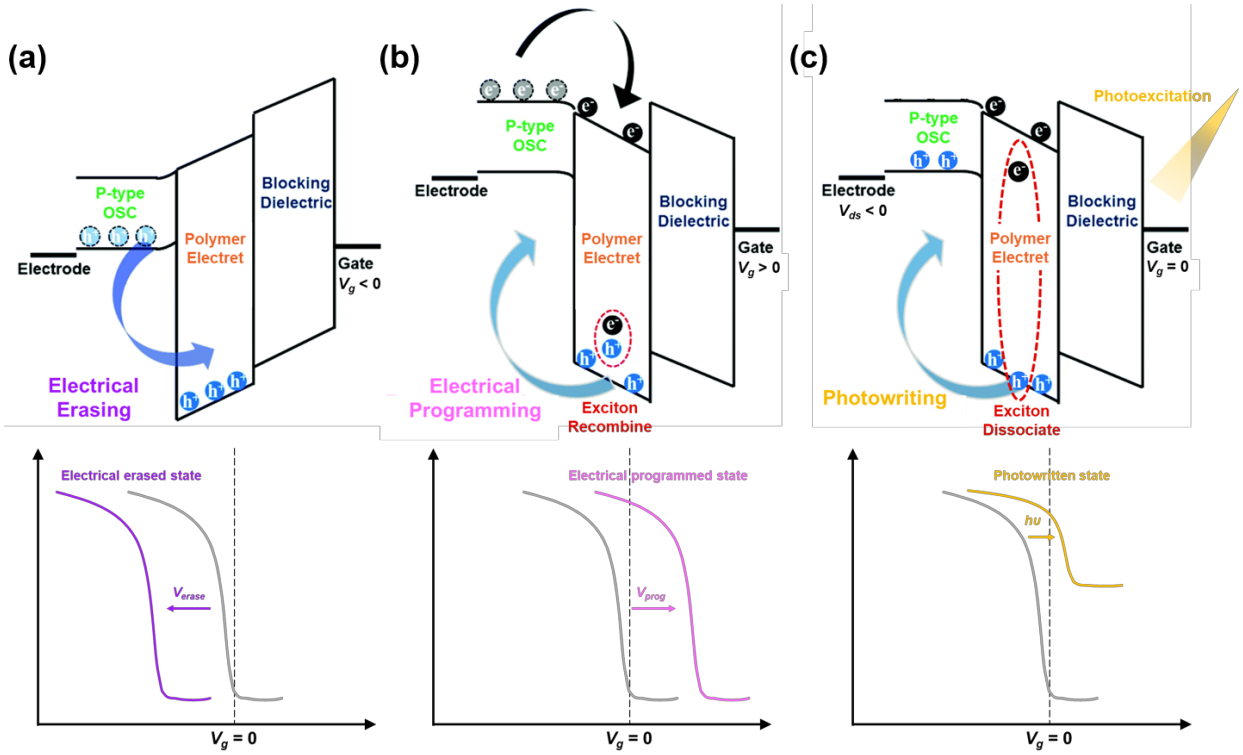

Fig. 2. Schematic illustrations of memory device operations and the corresponding shifting of transfer curves for the: (a) electrically erased state, (b) electrically programmed state, and (c) photowritten state.

3. Classes of polymer electrets for memory devices

3.1 Pendent sidechain polymer electrets

One effective strategy that has been employed to attain high charge-storage/trapping capabilities in polymer electrets is to attach strongly electronegative moieties to the pendent sidechains. Being the most electronegative element, fluorine has often been incorporated into the sidechains of polymer electrets for this reason. Some examples of polymers with highly fluorinated sidechains include poly(pentafluorophenyl acrylate) as well as trifluoromethylated and pentafluorosulfanylated styrenic polymers (Fig. 3). [23 – 26]

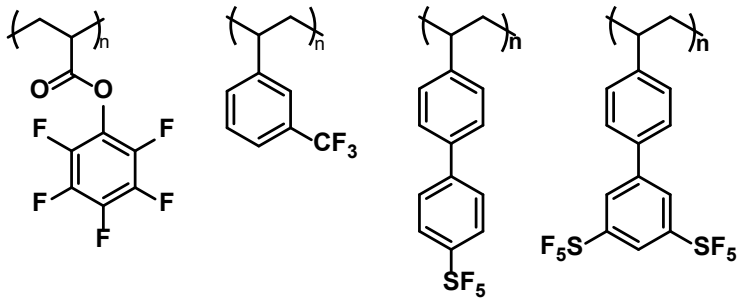

Fig. 3. Structures of polymer electrets with highly fluorinated pendent sidechains.

In 2020, Zhu et al. reported the synthesis and application of soluble atactic poly(4-fluorostyrene) (FPS) as a high-performance polymer electret in OFET-based memory devices. [27] In their study, FPS was synthesized by standard AIBN-mediated radical polymerization of 4-fluorostyrene (Scheme 1), which resulted in a polymer of M_w of 1,600 kDa and dispersity ($Đ$) of 1.25. The idea behind this polymer structure was to create an electret with long-term stability in its charged state, which translates into long-term memory stability. For their memory device studies, a pair of organic semiconductors, 2,7-didodecyl[1]benzothieno[3,2-b][1]benzothiophene (C12-BTBT) and poly[4-(4,4-dihexa-decyl-4H-cyclopenta[1,2-b:5,4-b0]dithophen-2-yl)-alt-[1,2,5]-thiadiazolo[3,4-c]pyridine] (PCDTPT), was used to form a C12-BTBT/FPS bilayer and PCDTPT/PS blend, respectively, to showcase the performance of FPS. Compared to a model polystyrene (PS) reference dielectric, FPS showed enhanced electron and

hole trap densities that were higher than PS by 29.6% and 9.6%, respectively, as well as an increased trap energy of over 0.1 eV. FPS also exhibited a larger water contact angle (97.3°) than did PS (86.6°), which points to the marked hydrophobicity typical of fluorinated polymers as a result of their lower surface energies. The enhanced hydrophobicity is thought to aid in preventing moisture from penetrating the material, thus improving long-term stability in air. Overall, FPS showed excellent performance as well as a record-high sheet charge density of 6.8×10^{12} cm^{-2}. In terms of device performance, a wide memory window of 108 V and a large on/off ratio of 10^7 were observed. The C12-BTBT/FPS transistor was also shown to be stable over 100 cycles of gate voltage scanning under ambient conditions. Another remarkable aspect of this study was the structural simplicity of FPS, which illustrates that desirable properties and optimal performance did not necessitate the use of complex molecular designs.

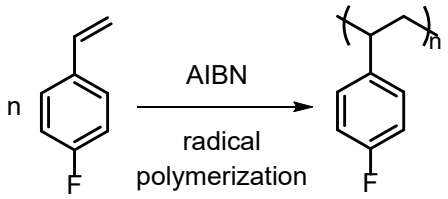

Scheme 1. Synthesis of FPS by AIBN-promoted radical polymerization.

Using a similar strategy of installing high-dipole-moment moieties on the pendent sidechains, a study by Xu et al. in 2023 reported the synthesis of four high-κ dielectric polymers featuring poly(methyl methacrylate) (PMMA)-type backbones with cyclic carbonates attached to the pendent sidechains via ester linkages. [28] The cyclic carbonate components were synthesized from the corresponding epoxides via reaction with carbon dioxide (Scheme 2). Subsequent radical copolymerization of methyl methacrylate, epoxide- and cyclic carbonate-functionalized monomers (with variable feed ratios) under the action of AIBN in DMF led to the desired target polymer electrets (Scheme 2). The polymers exhibited high κ values, good insulating properties, and amenability to solution processing. When in operation, the high-

dipole-moment carbonates on the polymers could redirect themselves under the action of the applied electric field and promoted stable device operation and efficient charge transfer. In OFET devices whereby the polymers were employed as the gate dielectric in floating-gate memories with embedded C_{60} nanoparticles in the charge memory layer, these cyclic carbonate-functionalized PMMA showed remarkable performance with large memory windows (8.5 V), stable retention (2×10^4 s), high on/off current ratios (10^3), cyclic endurance of 200 erase/write cycles, multi-level memories (> 4 levels), as well as non-destructivity. Operating at low voltage, the OFET devices showed mechanical robustness, negligible hysteresis behavior, high bias–stress stability, good environmental stability, and demonstrated applicability in one-transistor-one-transistor (1T1T) integrated memory cells.

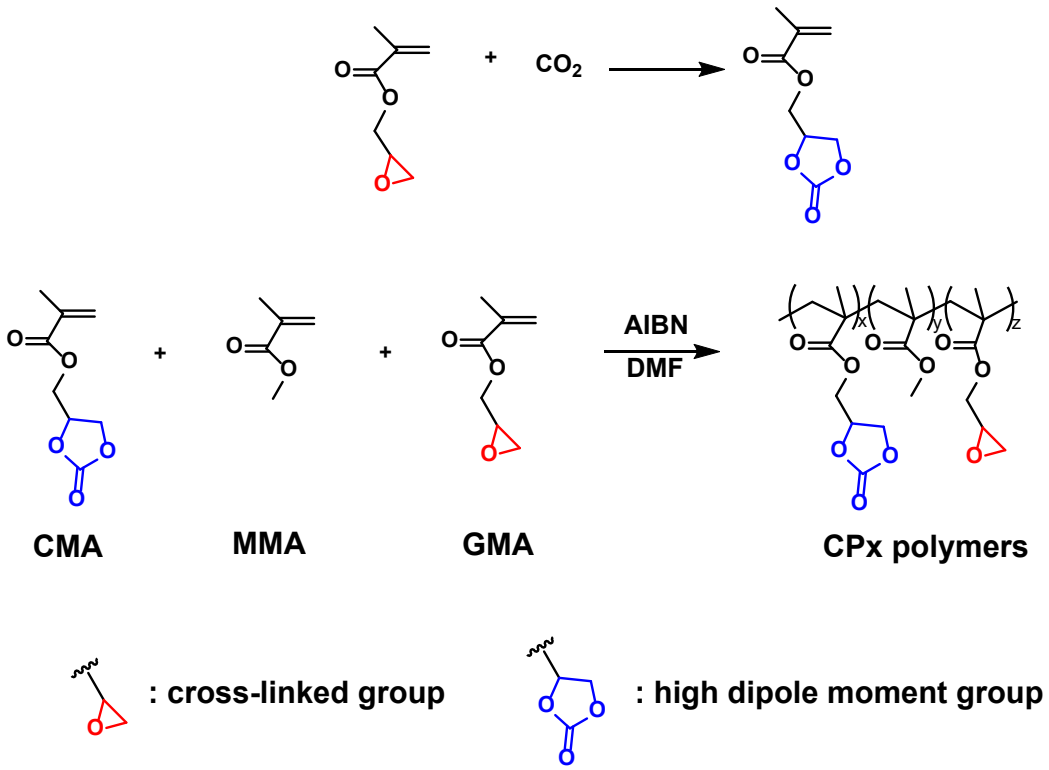

Scheme 2. Synthesis of cyclic carbonate-functionalized polymers via radical polymerization. Adapted with permission from ref. [28] (Copyright 2023 © Wiley-VCH Verlag GmbH & Co. KGaA, Weinheim).

While pendent polymers have mostly been used as stand-alone polymer electrets, a recent study by C.-L. Liu (a coauthor of this review), together with Lin and Chen, reported ultrahigh memory ratios with a supramolecular electret system comprised of porphyrin dyes, [29] namely *meso*-tetra(4-aminophenyl)porphine (TAPP), *meso*-tetra(*p*-hydroxyphenyl)-porphine (THPP), and *meso*-tetra-(4-carboxyphenyl)porphine (TCPP), hydrogen-bonded to poly(4-vinylpyridine) or poly(4-vinylphenol) (PVPh) (Fig. 4). With its pyridinic N lone pairs, the former pendent polymer can function as a hydrogen bond (H-bond) acceptor, while the latter polymer functions as a H-bond donor by virtue of its OH groups. For their memory devices, the authors employed the organic semiconductor dinaphtho[2,3-b:2′,3′-f]thieno[3,2-b]thiophene (DNTT) in conjunction with the dye/pendent polymer supramolecular system. While the strongly absorbing dyes acted as the ambipolar charge-trapping moiety, the insulating polymer electrets formed a barrier to stabilize the trapped charges in the H-bonded supramolecular structure. With this mixed dye/polymer system, it was determined that the hole-trapping ability of the device was a function of the electrostatic potential distribution in the supramolecular assembly. The supramolecular system with the more negative electrostatic potential showed stronger hole-trapping capability and a more negative threshold voltage of the electrically erased state. On the other hand, the electron-trapping ability depended on the acidity and interfacial interactions. The positively-charged protons served as the electron trapping sites, and they enhanced the dissociation of the excitons and the transfer of the free hole carriers. Of the different polymer/dye combinations, the optimally H-bonded PVPh:TCPP showed the largest memory ratio of 1.12×10^8 over 10^4 s, which was the best reported performance as of the time of the study. Overall, the use of this supramolecular pendent polymer electret/porphyrin dye system showed good reliability, switching endurance, and discernability in long-term stability for phototransistor memory device applications that call for fast programming/readouts and distinguished memory ratios. Lastly, the reported binary

pendent polymer/dye system also offers modularity and tunability in that the component structures could be fine-tuned according to structure-property relationship guidelines for the purpose of creating superior low-energy consumption photonic electronics in the future.

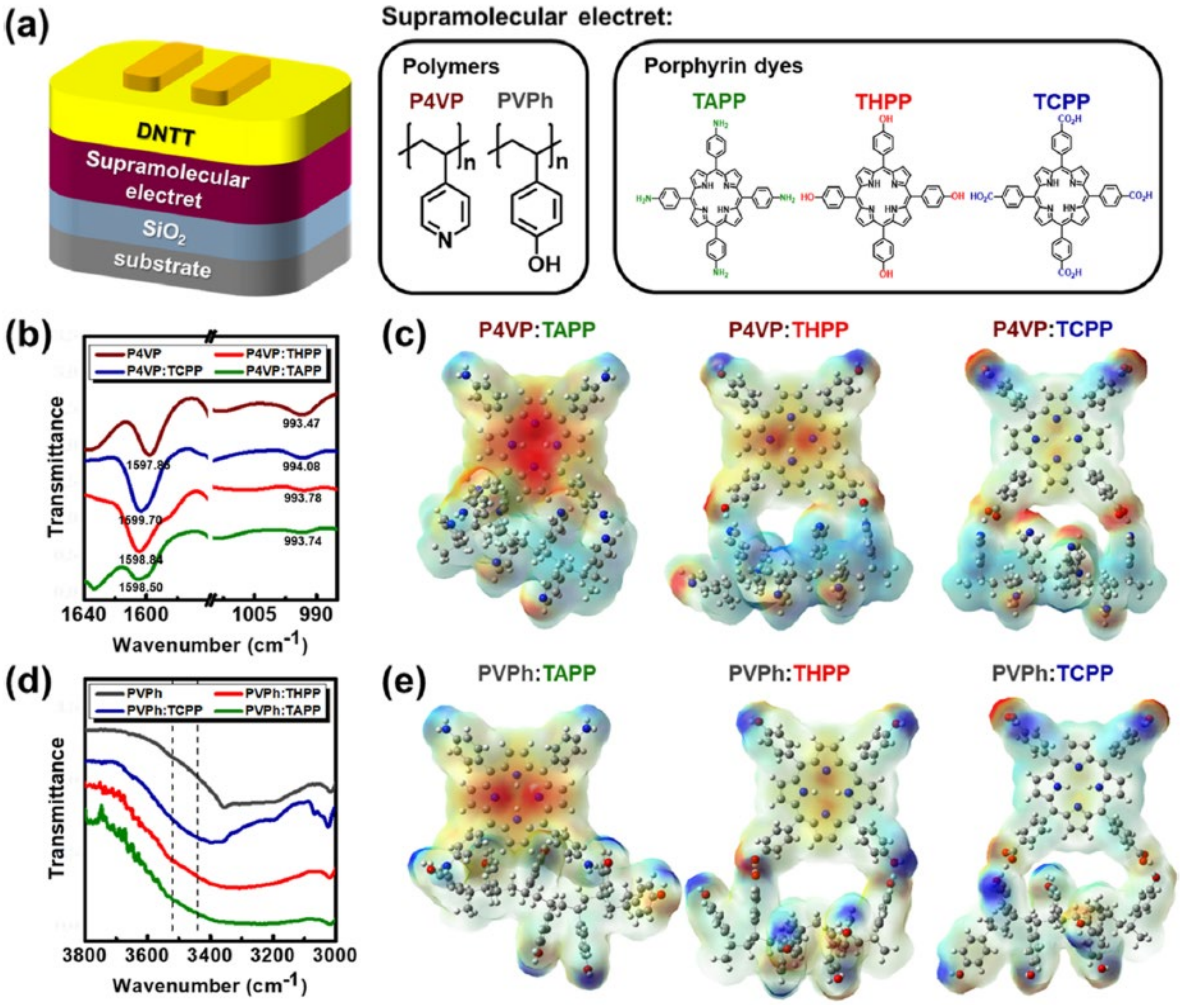

Fig. 4. (a) Schematic diagram of the phototransistor memory device and the chemical structures of its constituent materials. (b,d) FT-IR spectra and (c,e) ESP mappings of the supramolecular assemblies based on (b,c) poly(4-vinylpyridine) and (d,e) poly(4-vinylphenol) H-bonded to various porphyrins (TAPP, THPP, TCPP). Reprinted with permission from ACS Appl. Mater. Interfaces, 15 (2023) 19258. [29]. Copyright 2023 American Chemical Society.

In spite of pendent polymers being so popularly studied in polymer electret-based OFET memory devices, the effects of polymer molecular weight on the electret's charge-

trapping ability remains incompletely understood. Elucidating this relationship proved to be an interesting line of inquiry investigated by Wang et al. in their recent 2023 work involving poly(*N*-vinylcarbazole)-based electrets [30]. The chemical structure of poly(*N*-vinylcarbazole) comprises a nonconjugated aliphatic backbone and carbazole heterocycles as the pendent sidechains (Fig. 5). As an optoelectronic material, the polymer displays unique hole-transporting capabilities and optical properties, and it has been utilized as a continuous floating-gate electret in light-programmable/erasable OFET-based memory devices.[31, 32]

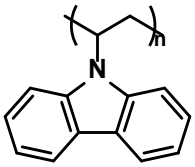

Fig. 5. Chemical structure of poly(*N*-vinylcarbazole) used in the study by Wang et al. [30]

Generally, it is known that the performance parameters (e.g., operation speed, memory window, retention, endurance, etc.) of memory devices are intimately related to the molecular structure of the polymer electret as well as the nature of the electret/semiconductor interface. Significant work has gone into investigating the structure-property-function relationships between polymer electrets and their memory performance. Multiple contributing factors such as intramolecular/intermolecular charge transfer, [33–34] π-conjugation length, [35–37] polymer chain aggregation,[38,39] hydrophobicity/hydrophilicity,[40] morphology and film thickness,[41,42] have all been studied. Invariably, all these parameters are able to influence charge-transport and charge-trapping characteristics in profound ways. In contrast, there have been no systematic studies of the effect of polymer electret molecular weight on its charge-trapping ability in OFET memory devices. In their 2023 study, Wang et al. investigated pentacene-based synaptic OFET memory devices fabricated from poly(*N*-vinylcarbazole) electrets of two different molecular weights (90 kDa and 1,100 kDa). Interestingly, the OFET

memory device made from lower molecular weight polymer electret exhibited faster write speed (1 ms) and larger memory window (28.2 V) than the device made with higher molecular weight polymer. The enhanced performance is thought to be due to the smoother surface morphology, higher polymer chain-end density, larger tunneling electric field strength, and superior charge-trapping ability of the lower molecular weight poly(*N*-vinylcarbazole). This work has led to an improved understanding of the effect of polymer molecular weight on charge-trapping behavior OFET-based memories. Nonetheless, additional structure-property relationship studies will still be needed if a comprehensive understanding of how to rationally design high-performance polymer electrets is to be achieved.

3.2 π-conjugated polymers

Another major class of polymers that has often been used as electrets in OFET-based memory devices are the π-conjugated polymers. Compared to the fully saturated polymers discussed in the previous section, π-conjugated polymers feature unsaturated molecular structures whereby mutual π-orbital overlap and electronic communication is maintained along the length of the polymer backbone. Apart from this intrachain characteristic, nonbonding interactions between polymer chains such as π-π stacking are also typical. The careful design and modification of the π-conjugated polymer structure allows for fine-tuning of the energy-level alignments between the semiconductor and polymer electret layers in memory devices. The charge-trapping process can be facilitated through the π-conjugated backbone, which in turn modulates the memory performance of the device. Besides being electroactive, π-conjugated polymers are typically also photoactive (i.e., light-responsive), which introduces an additional orthogonal option for implementing the programming function of the transistor. Photo-modulated transistor memory facilitates high-speed optical signal transfers with less noise and requires less energy to operate. [13] An example would be the carbazole-containing

π-conjugated polymers. [43] These electron-rich carbazole polymers have shown promising results as electret materials because of their unique optoelectronic properties featuring shallow excited triplet states that could be useful for both electronic and photonic devices. Their properties can be controlled through various strategies such as modifying the π-conjugation length or by introducing electron-accepting moieties. [1] In 2020, Chen et al. designed highly photoresponsive carbazole-based ABAB-type π-conjugated polymer electrets containing electron-rich 1,8-carbazole units as the donor groups and bithiophene/benzothiazole moieties as the comonomer units (Fig. 6). [44]

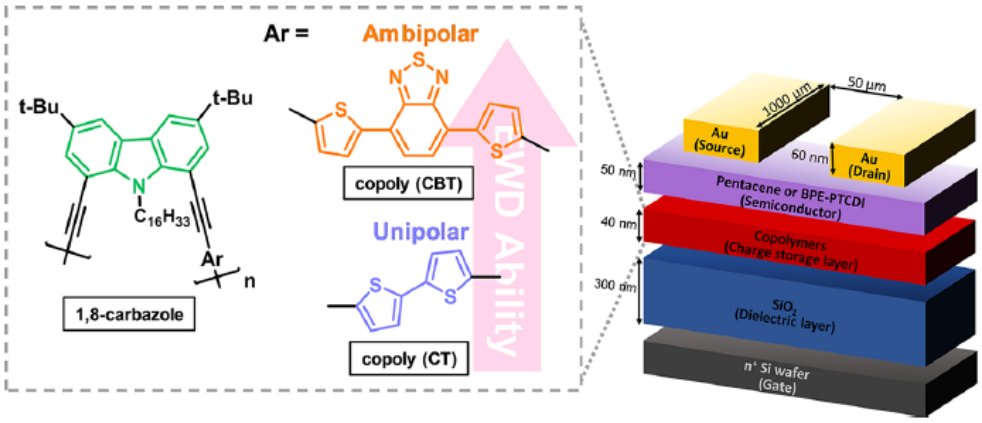

Fig. 6. Schematic of an OFET-based memory device fabricated with carbazole-containing π-conjugated polymer electrets, copoly(CT) or copoly(CBT). Reprinted with permission from ACS Appl. Mater. Interfaces, 12 (2020) 6144 - 6150. [44] Copyright 2020 American Chemical Society.

As expected, both π-conjugated polymers showed efficient visible-light absorption and photoluminescence quenching in their film states, which indicated formation of a substantial number of non-emissive excitons. However, compared with copoly(CT), the alternating donor-acceptor structure of copoly(CBT) showed superior photosensitivity and photo-recovery responses as a result of charge stabilization through enhanced separation of excitons (electron−hole pairs). The excitons generated by the twisted donor−acceptor moieties could

also be efficiently dissociated into free charges via charge delocalization. A donor-acceptor structure also comes with the potential for ambipolar charge-trapping behavior that promotes both electron and hole capture. The unique ambipolar trapping property of copoly(CBT) made it possible to achieve three-level data storage, thus expanding the storage density of the device. In regard to *p*-type OFET memory of the copoly(CBT)-based device, a memory window as wide as 49 V could be obtained when a programming voltage of –90 V (1 s) was used. The device was able to maintain the off-state for ~10^5 s with an on/off ratio of about 10^3. Furthermore, the endurance of copoly(CBT) was demonstrated over 50 switching cycles and the device was shown to operate stably with no apparent degradation.

In 2023, utilizing a similar theme of donor-acceptor repeating structures, Yang et. al. designed crosslinked core−shell nanoparticles made up of donor−acceptor type π-conjugated polymers and used them as floating-gate electrets in phototransistor memories. [45] The outer shell of the nanostructure was composed of hydrophilic poly(ethylene glycol) methyl ether methacrylate (PEGMA), while the inner core comprised of π-conjugated polymers with various repeat units: electron-donating thiophene (T) and bithiophene (2T) moieties, and electron-accepting benzothiazole (BT), naphthalenediimide (NDI), and hexafluorobenzene-naphthalenediimide (FB-NDI). Using different combinations of these molecular building blocks, four types of π-conjugated core structures were synthesized (Fig. 7).

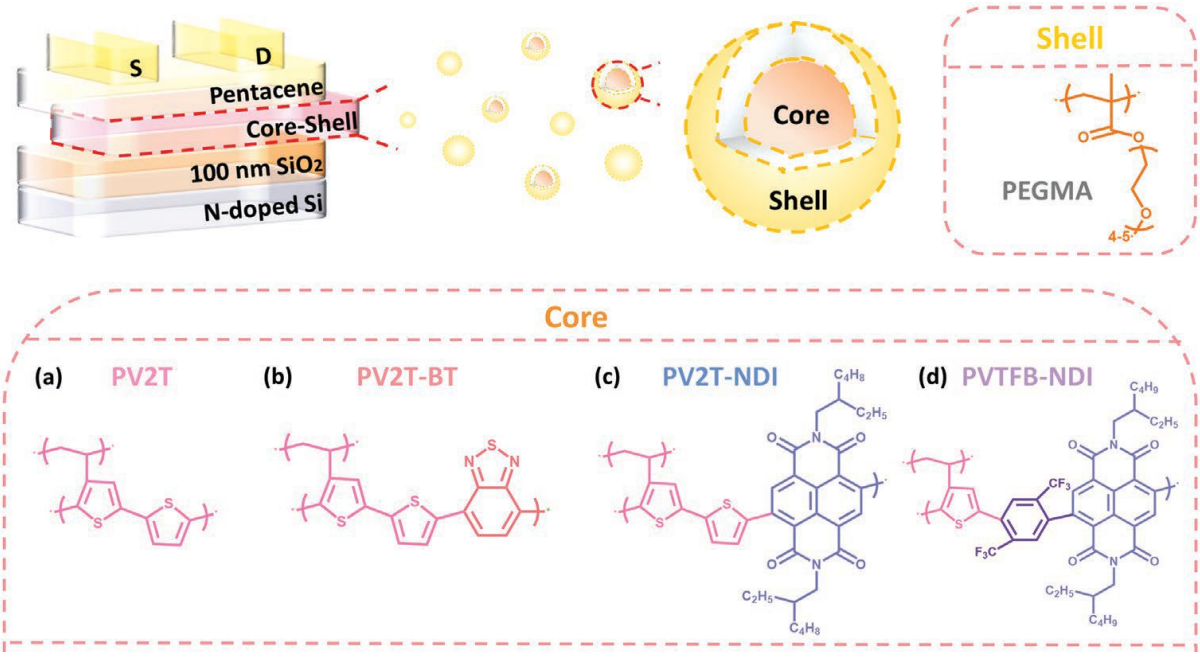

Fig. 7. Schematic of the phototransistor memory device and the structures of the donor-acceptor π-conjugated polymers that form the crosslinked core-shell nanoparticles. Adapted with permission from ref. [45] (Copyright 2022 © Wiley-VCH Verlag GmbH & Co. KGaA, Weinheim).

The donor−acceptor type nanoparticles demonstrated better electron-trapping ability than the donor-only PV2T nanoparticles. It was also observed that uniform core-shell nanoparticles had favorable charge-trapping performance due to the homogeneous isolation between the π-conjugated cores and the channel. The optimized core-shell structure of the PV2T-BT electret prevented charge-recombination through direct contact with pentacene and helped maintain electron-trapping. The core structures PV2T-BT and PV2T-NDI displayed much higher ON-state current than PV2T and PVTFB-NDI while the OFF-state current associated with all structures were similar, thus demonstrating the effectiveness of electron-trapping. In terms of endurance performance, the phototransistor based on optimized PV2T-BT-based crosslinked nanoparticles gave the highest memory ratio of 10^5 over 10^4 s at an operating voltage of −40 V. It also exhibited the highest paired-pulse facilitation index of 168%

at an operating voltage of −1 V, plus ultralow energy consumption of only 0.0324 fJ at an operating voltage of −1 μV. In brief, this study by Yang et al. showed that the core−shell and donor−acceptor designs were key to enhancing their charge-trapping, photoresponse, and overall phototransistor-based memory performance.

In other recent work spearheaded by Lee and Chueh, the researchers reported the synthesis and application of ambipolar π-conjugated polymers in floating gate-free memory devices. [46] This work differentiates itself from preceding examples in that the π-conjugated polymer functions as both the organic semiconductor and the electret. In other words, the polymer is capable of concurrent charge transport and storage, which is important for the function of synaptic transistors. For this, five dual-acceptor polymers were synthesized via the random copolymerization of diketopyrrolopyrrole- and benzotriazole-containing monomers using varied molar ratios of each building block. The structures of these resulting polymers are shown in Fig. 8. It was found that as the content of the benzotriazole component was increased, the UV-vis absorption peak of the polymers became gradually blue-shifted from 675 nm to 590 nm, suggesting that greater structural randomness was disrupting the interchain packing and this was one way in which the energy levels could be fine-tuned. After closer investigation, the authors were also able to establish clear structure-property relationships in regard to hole/electron ratio, memory retention, and synaptic behavior for their floating-gate free transistor. They found that polymers with balanced ambipolarity showed superior charge-trapping abilities and larger memory windows. This was a trade-off, however, as high ambipolarity (e.g., F0) also gave rise to higher volatility in terms of memory characteristics, i.e., poor memory retention. In contrast, the π-conjugated polymer with lower ambipolarity (e.g., F40) showed better memory retention ability but a smaller memory window. Polymer F40 thus presented with the most pronounced artificial synaptic characteristics. In conclusion,

this study on floating-gate free transistor-based memories highlighted the relationship between the polymer channel's ambipolarity and the resulting memory characteristics and synaptic behaviors, thus providing a clear design principle for the fabrication of future devices.

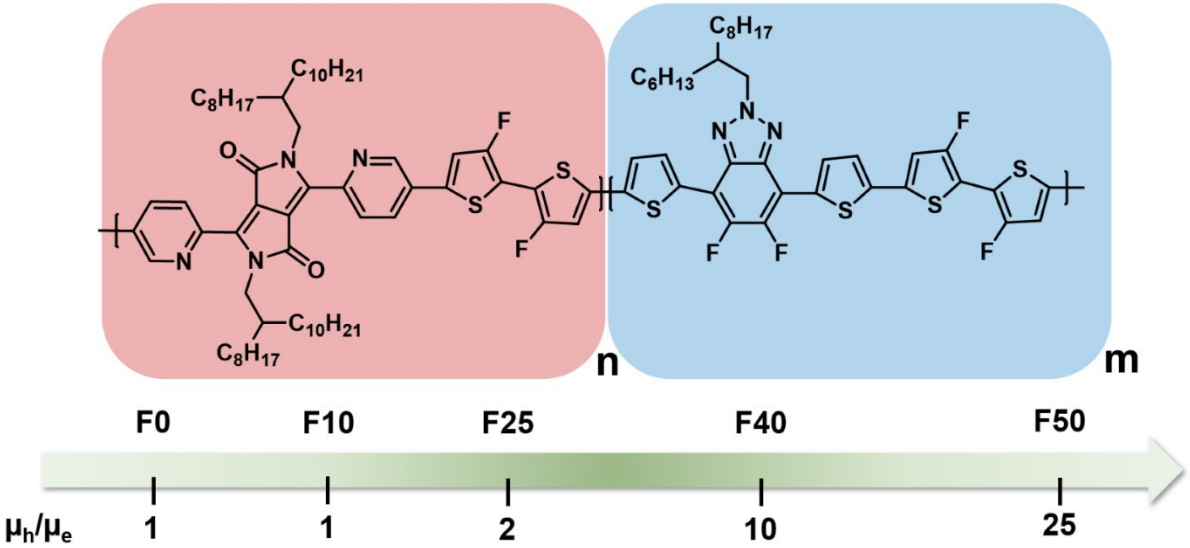

Fig. 8. Chemical structures of the π-conjugated polymer series F0–F50 containing diketopyrrolopyrrole and benzotriazole units. Adapted with permission from ref. [46] (Copyright 2022 © Wiley-VCH Verlag GmbH & Co. KGaA, Weinheim).

In this final example on π-conjugated polymer electrets, we show that useful properties from a different sub-area of materials chemistry, i.e., aggregation-induced emission (AIE), can also be harnessed for organic memory applications. The AIE phenomenon refers to organic luminophores that possess enhanced emission behavior in their aggregated state compared to the solution phase. In the context of organic photonic memory devices, researchers have unsurprisingly found these AIE properties to be very useful. In 2021, Ke et al. [47] developed AIE-active π-conjugated polymer electrets for high-performance photoprogrammable memory applications. Three polymers PTPA-CN, PTPA-CNBr, and PTPA-3CN were prepared, all of which were structurally based on triphenylamine donor moieties connected to cyano-

functionalized acceptor motifs (Fig. 9). The first two polymers were observed to be highly fluorescent and AIE-active, while PTPA-3CN was nonfluorescent and regarded as an aggregation-caused quenching (ACQ) polymer.

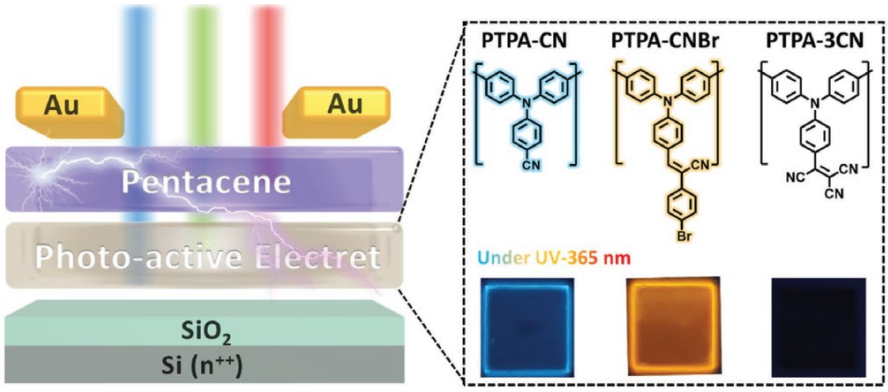

Fig. 9. Schematic representation of the reported photoprogrammable recorder device, and the molecular structures of the AIE-active polymer electrets and their luminescence properties. Adapted with permission from ref. [47] (Copyright 2021 © Wiley-VCH Verlag GmbH & Co. KGaA, Weinheim).

The photonic memory devices fabricated with the AIE-active polymers showed ultrafast programming times of 0.1 ms, high current on/off ratios of up to 10^5 and 10^6 (for PTPA-CN and PTPA-CNBr respectively), and long retention times of over 40,000 s with no appreciable dissipation. Photoprogrammable behavior was attained by engineering the proper energy level alignment between the pentacene semiconductor and the polymer electret, thus promoting dual-layer excitation upon continuous irradiation. Moreover, enhancement of the memory window could also be achieved since the semiconductor was able to absorb light emitted from the AIE-active polymers efficiently enough to produce more excitons. In comparison, the nonfluorescent ACQ polymer (PTPA-3CN) exhibited mismatched energy levels with pentacene and was found to suppress the photoresponse effect, resulting in no recorded output current signals. Hence, the study showed that rational molecular design could be leveraged to engineer the energy levels between semiconductor and electret to create high-

performance photonic memory devices. The findings therein are expected to pave the way towards the systematic design of next-generation π-conjugated polymer electrets for ultrafast optical storage applications.

3.3 Block copolymers (BCPs)

In addition to the π-conjugated systems and nonconjugated pendent polymers described in the preceding two sections, BCPs that incorporate both types of structures have also been employed as electrets, particularly in photonic FET memory devices. While it is possible to use blends composed of nonconjugated and π-conjugated polymers, miscibility and unfavorable phase separation issues are commonly encountered due to inherent differences in their physicochemical characteristics. For instance, W.-C. Chen and coworkers were the first to demonstrate the utility of a π-conjugated/insulating blend of poly(2,7-(9,9-dioctylfluorene)) (PFO) and PS as an electret in a high-performance photonic FET memory device featuring fast multilevel photonic response. [1] While the optimized interface between the physically blended conjugated polymer and insulating polymer was able to facilitate the transfer of photo-induced charge carriers, the aforementioned miscibility problems are known to compromise overall device performance. For that reason, Chen et al. subsequently developed a BCP system based on PFO-*b*-PS as the floating-gate electret in a photonic FET-based memory device. [48] The BCPs were synthesized through facile click chemistry whereby an alkyne-terminated PFO was covalently linked to an azide-terminated nonconjugated PS chain via Cu(I)-catalyzed Huisgen [3+2] cycloaddition to afford a diblock copolymer (Scheme 3).

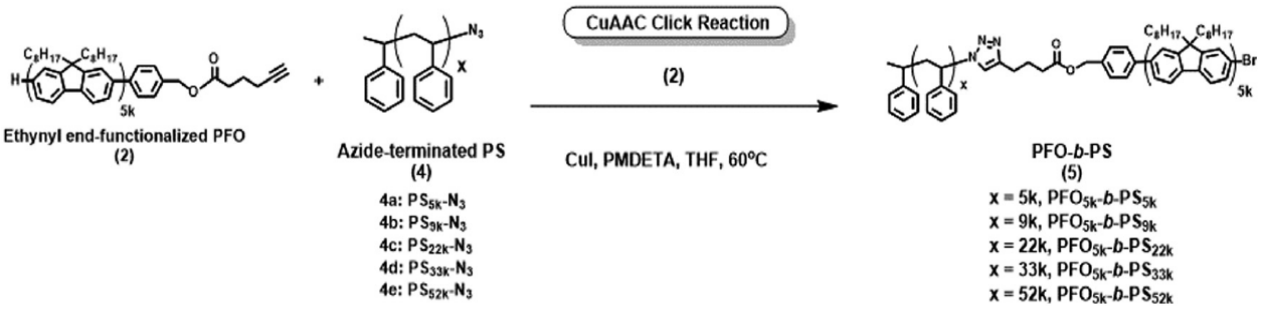

Scheme 3. Synthesis of PFO-*b*-PS electrets via copper(I)-catalyzed click chemistry. Reprinted from ref. [48] with permission from The Royal Society of Chemistry.

The π-conjugated PFO was pre-synthesized by Suzuki-Miyaura polycondensation while azide-terminated PS of different molecular weights were prepared by ATRP. This modular synthetic approach allowed BCPs with varying PS content to be made readily. The resulting memory device based on this PFO-*b*-PS electret system showed dynamic switching behavior in its photo-writing and electrical-erasing processes. As the π-conjugated component, substituted polyfluorenes have been preferred by Chen et al. due to their favorable energy levels, semiconducting nature, photoactive response attributes, and versatility in fine-tuning their properties based on alkyl substituent choice. In this study, the authors noted that BCPs with higher PS content afforded superior device performance, possibly due to better electron-trapping ability resulting from enhanced *β*-conformation of the PFO, as well as stabilization of those electrons due to the intimately microphase-separated morphology at the PFO/PS interface. However, further increasing of the PS content led to reduced photoresponse, which is due to the decreased relative content of the electron-trapping PFO moieties. Ultimately, it was found that PFO_{5k}-*b*-PS_{22k} was optimal on the basis of its high current on/off ratio of 10^4 and long retention time of over 10,000 s.

Apart from the PFO-*b*-PS system detailed above, Chen et al. have also reported other polyfluorene-containing BCPs featuring other types of nonconjugated polymer segments. In 2021, Chen and Satoh described a series of π-conjugated/insulating BCPs based on poly(9,9-

di-*n*-hexyl-2,7-fluorene)-*b*-poly(δ-decanolactone)s (PF-*b*-PDL$_x$, x = 1−3) as stretchable hole-trapping materials in OFET memory devices. [49] Compared to PFO-*b*-PS, PF-*b*-PDL$_x$ featured shorter alkyl chains on the conjugated segment and a polyester rather than polyolefin backbone as the nonconjugated block. Likewise, the chemical synthesis of these target polymers relied on Huisgen cycloaddition-based click chemistry whereby alkyne-terminated PF was bonded to an azide-terminated PDL bearing 1–3 branches (Scheme 4). The two requisite homopolymer blocks were first pre-synthesized through modified Suzuki-Miyaura polycondensation and living ring-opening polymerization, respectively.

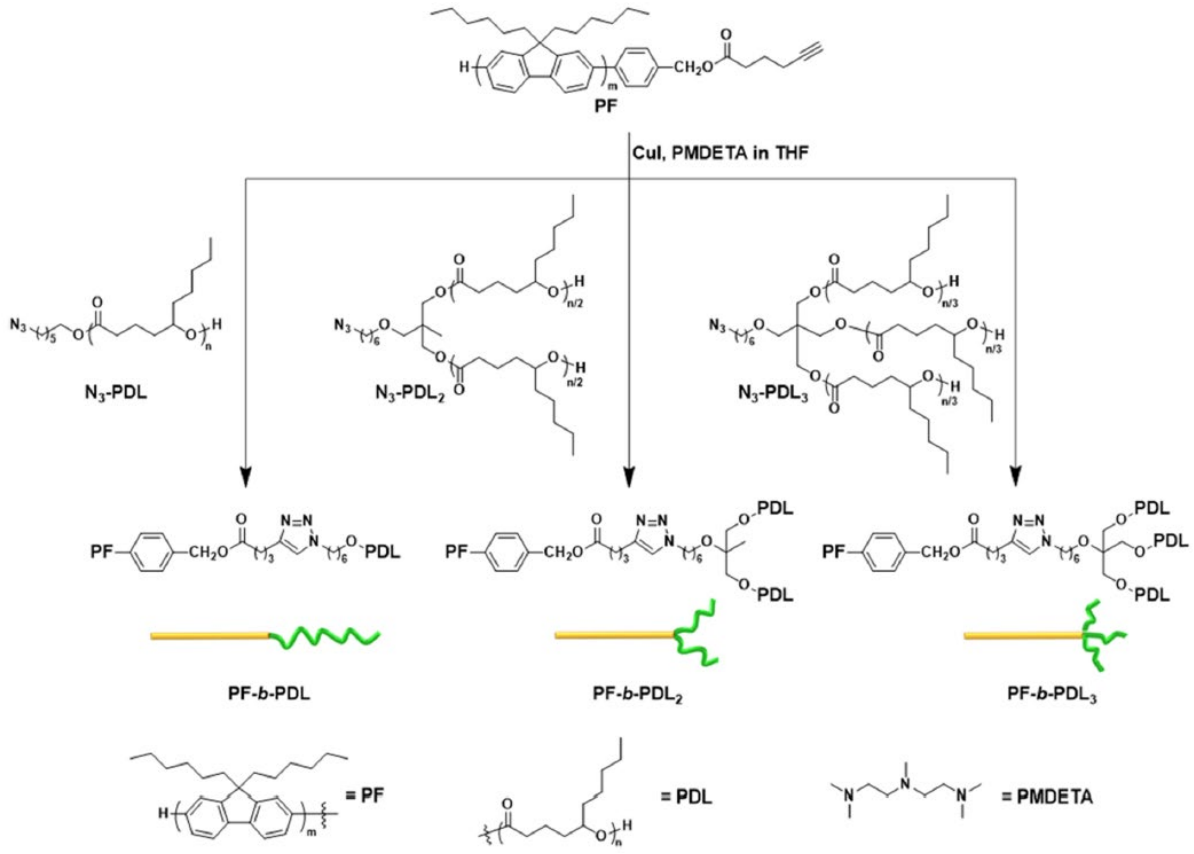

Scheme 4. Synthesis of PF-*b*-PDL, PF-*b*-PDL$_2$, and PF-*b*-PDL$_3$ via Cu(I)-catalyzed azido–alkyne click reactions. Reprinted with permission from ACS Appl. Mater. Interfaces, 13 (2021) 2932. [49] Copyright 2021 American Chemical Society.

The idea behind this BCP molecular design was to create an intrinsically flexible and stretchable material that could also trap charges. The use of linear and branched nonconjugated PDL blocks provided a means to examine the effect of polymer architecture on morphology as well as device performance. It was found that the branched PDL-based soft segments improved stretchability and also enabled the crystallinity and microphase separation within the BCPs to be tuned, which enhances the charge-trapping ability. Among the three BCPs investigated, the authors found that using PF-*b*-PDL$_3$ as the electret layer afforded the OFET memory device with the largest memory window (i.e., 102 V), highest memory ratio (i.e., 3.5×10^4), and highest hole-trapping density (7.3×10^{12} cm^{-2}). The device was even able to retain its performance under 100% strain. To elucidate why this was the case, differential scanning calorimetry studies were performed, which showed that the π-conjugated PF blocks linked to branched BCPs crystallized more homogeneously than those linked to linear BCP, which afforded a more uniform PF crystalline phase instead. Atomic force microscopy measurements also showed that the BCPs with branched PDL formed longer PF nanofibers with larger coverage areas, which in turn provided superior memory device performance. In the retention test, the memory ratio decayed more rapidly as the number of branches of PDL decreased. This suggests that the PDL segments can block the hole carriers in PF and prevent them from being detrapped, which in turn augments the retention performance. Finally, an added advantage of PDL is that it is biobased, making it potentially greener and more sustainable than petroleum-derived alternatives.

Using the same PF/insulating polymer diblock copolymer design, it has also been possible to introduce additional properties and capabilities into the electret material through the strategic choice of the nonconjugated component. Examples of such extra features include multiband photoresponsive and thermoresponsive capabilities, as demonstrated by Chen and coworkers in 2021 and 2023, respectively. [50, 51] In the earlier study, the authors showed that

by pairing up poly[2,7-(9,9-dihexylfluorene)] with poly(pendent-isoindigo) (Piso), the resulting PF-*b*-Piso exhibited multiband photoresponse in a photonic FET memory device. [50] This ability is derived from the absorption properties of the isoindigo moieties in the Ultraviolet C range (UVC, 200–280 nm), in addition to the microphase separation and self-assembly abilities of analogous BCPs, as discussed above. In terms of performance, the memory device based on pentacene and PF-*b*-Piso$_{20}$ (Fig. 10) showed high current contrast of 10^6 and 10^5 over 10^4 s in response to 405 nm and 254 nm light, respectively. A current contrast of 10^2 and 10^4 was also attained in response to 530 and 650 nm light respectively, as a result of charge-transfer between the channel and memory layers. Furthermore, the memory device also demonstrated remarkable long-term stability and switching endurance, i.e., memory ratios of 10^6 were maintained over 10^4 s in the retention test and 10^4 for ten WRER cycles under 405 nm light.

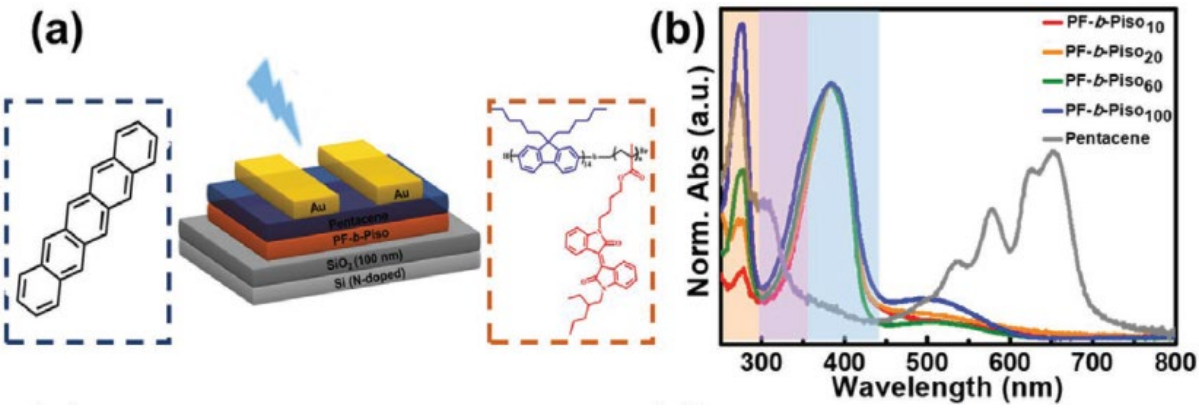

Fig. 10. a) Device architecture and the chemical structures of the block copolymers in the channel and memory layers. b) UV–vis absorption spectra of pentacene and PF-*b*-Piso. Adapted with permission from ref. [50] (Copyright 2021 © Wiley-VCH Verlag GmbH & Co. KGaA, Weinheim).

In the subsequent work, Chen et al. combined PF with poly(*N*-isopropylacrylamide) (PNIPAAm) in a diblock copolymer to produce an electret system with thermoresponsive photomemory properties. [51] PNIPAAm itself is a well-known thermoresponsive polymer due

to its lower critical solution temperature (LCST) of 30−33 °C.[52] Chemically, each repeat unit of PNIPAAm features a pendent amide moiety, which presents multiple hydrogen-bonding sites. Variations in its hydrogen-bonding and hydrophobic interactions allow the polymer to undergo rapid and reversible conformational reorganizations during heating/cooling. By synthesizing a BCP that incorporates both PF and PNIPAAm segments, the authors were able to create an electret system with photoactive as well as insulating and thermoresponsive properties. In the study, a series of PF-*b*-PNIPAAm diblock copolymers with varying PF and PNIPAAm content was synthesized (Fig. 11), and their thermal and optical properties were systematically optimized. For the photomemory device, these multifunctional BCPs were used as the electret while 2,7-dioctylbenzothieno[3,2-b1]benzothiophene (C8-BTBT) was employed as the semiconductor. Subsequent structure−performance studies showed that the optimized device utilizing PF-*b*-PNIPAAm (7-188) electret exhibited ambipolar charge-trapping abilities, showing a memory ratio of $\sim 10^5$ and a large memory window of about 23.12 V. Notably, the photomemory device had enhanced data retention stability at 40 °C due to conformational reorganization of the BCP and consequent charge-trapping variation due to resistivity changes. At this temperature, the PNIPAAm blocks undergo chain reorganization via hydrogen-bonding interactions, leading to aggregation of the PF blocks which retards charge-trapping in the PF-*b*-PNIPAAm. Consequently, the PF-*b*-PNIPAAm electret showed slow charge relaxation at an elevated temperature and demonstrated enhanced memory stability for over a year. This work further highlighted the versatility and modularity of π-conjugated/nonconjugated BCP systems in that any desired functionality could be rationally incorporated into a polymer electret to bring about certain performance characteristics. Potential areas of utility for BCP-based electrets include nonvolatile memory applications and photosynapses in neuromorphic computing.

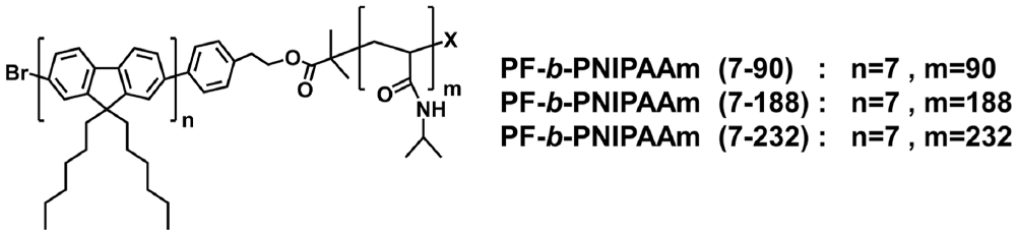

Fig. 11. Chemical structures of the PF-*b*-PNIPAAm series of BCP electrets. Adapted with permission from ACS Appl. Polym. Mater., 5 (2023) 463. [51] Copyright 2023 American Chemical Society.

Departing from the π-conjugated/nonconjugated diblock copolymer template, Chen et al. also demonstrated that BCPs with *two* nonconjugated backbones could be employed in high-performance nonvolatile phototransistor memory devices. [53] In this case, one of the nonconjugated polymer blocks was decorated with π-conjugated moieties (i.e., pyrene) on its pendent sidechains, as opposed to the entire polymer block being fully π-conjugated. Specifically, the authors reported a series of dual-functional BCP electrets based on the poly(ethylene oxide)-*block*-poly(1-pyrenemethyl methacrylate) (PEO-*b*-PPyMA) system and studied the effects of molecular design and self-assembled morphology on the resulting phototransistor memory characteristics. The rationale behind their polymer design was that PPyMA would function as the photogate while the PEO could boost charge stability via electrostatic interactions. To prepare the BCPs, the photoactive PPyMA component was first synthesized via ATRP using an initiator bearing an alkyne moiety (Scheme 4). Following this, an azide-terminated PEO was then attached to the PPyMA via click chemistry based on the Huisgen [3+2] cycloaddition. This modular synthetic route allowed a series of BCPs with varied PPyMA and PEO compositions to be easily obtained. The BCPs were subjected to solvent-annealing so as to promote self-assembly into ordered vertical cylinder nanostructures. Properties-wise, the BCP electrets exhibited excellent charge-trapping and stabilization capabilities in devices featuring pentacene as the organic semiconductor. The phototransistor

memory device containing solvent-annealed PEO_{5k}-*b*-$PPyMA_{10.2k}$ as the electret afforded a wide memory window (54 V), excellent memory stability (>10^6), and rapid multilevel photoresponse (200 ms). The pyrene moieties, which were likely π-stacked extensively following self-assembly, were believed to aid in the accumulation of charges (i.e., holes transferred from pentacene). The PEO component, on the other hand, possesses lone pairs on its oxygen atoms that could stabilize the holes. Moreover, the self-assembled morphology of the BCP electret induced by solvent-annealing is conducive to the localization of the functional regions, leading to the improved memory performance over the non-annealed devices. Overall, the structure–morphology–performance relationship in these intrinsic dual-functional BCPs hinge on the synergy between the two constituent blocks. The ease with which each of the constituent blocks in the BCPs may be tailored makes such a system promising as custom electrets for next-generation high-performance memory applications.

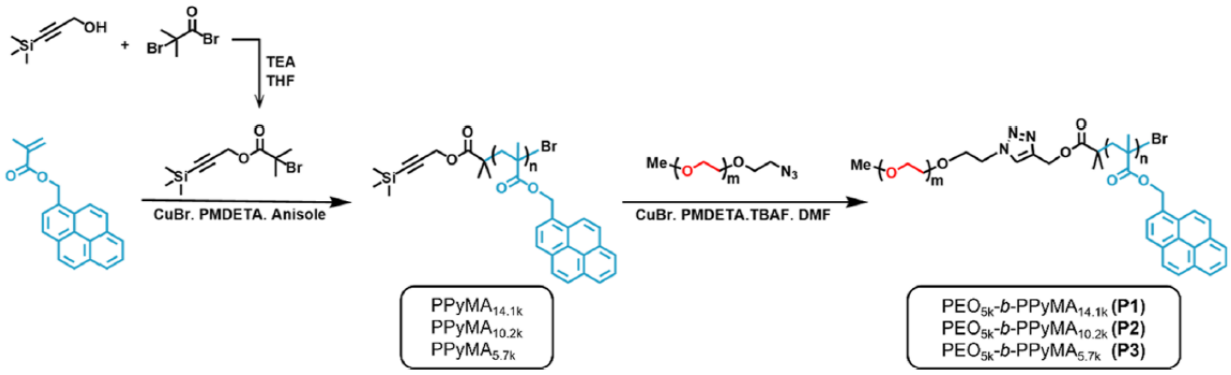

Scheme 4. Synthesis of the PEO-*b*-PPyMA diblock copolymer electrets. Reprinted with permission from Macromolecules, 55 (2022) 8262. [53] Copyright 2022 American Chemical Society.

3.4 Other polymeric systems

In this section, the focus will be on several recent advances in the development of miscellaneous polymer electret systems that fall outside the abovementioned categories of materials or incorporate elements from multiple categories. These include hybrid systems

containing both π-conjugated and nonconjugated segments, all-organic composite systems, partially π-conjugated polymers with donor-acceptor backbones and AIE properties, and sustainability-inspired biodegradable and/or biobased electret materials. In all cases, the common themes were interdisciplinarity and the ability of the researchers to leverage know-how from different sub-areas of materials chemistry to create multifaceted organic (photo)memory technologies.

One especially noticeable trend that has emerged across various research fields is the push towards sustainability. For example, in the area of organic-based digital data storage technologies, it has recently become popular for researchers to develop and employ renewable polymers in place of petroleum-derived ones. [54–57] One recent piece of work exemplifying this trend came from Chen and coworkers, [54] who reported the sustainable development of degradable materials for photonic memories from renewable biomass-derived precursors. Specifically, the authors synthesized a series of photoactive biobased poly(azomethine)s (PAMs) with degradable imine and ester linkages and demonstrated their utility as chargeable electrets for organic phototransistor memories. Three PAMs (**P1**−**P3**) were synthesized via the condensation polymerization of a biomass-derived diamine, (3R,6S)-hexahydrofuro[3,2-b]furan-3,6-diyl bis(4-aminobenzoate) (ISBA), with a pair of dialdehydes, namely, the photoactive 9,9-di-n-octylfluorene-2,7-dicarboxaldehyde (FLDA) and the biobased 2,5-furandicarboxaldehyde (FCA), as shown in Scheme 5a. For comparison, a fourth polymer (**P4**) without imine linkages was also prepared via Pd-catalyzed Suzuki polycondensation from the corresponding dibromide and diboronate (Scheme 5b).

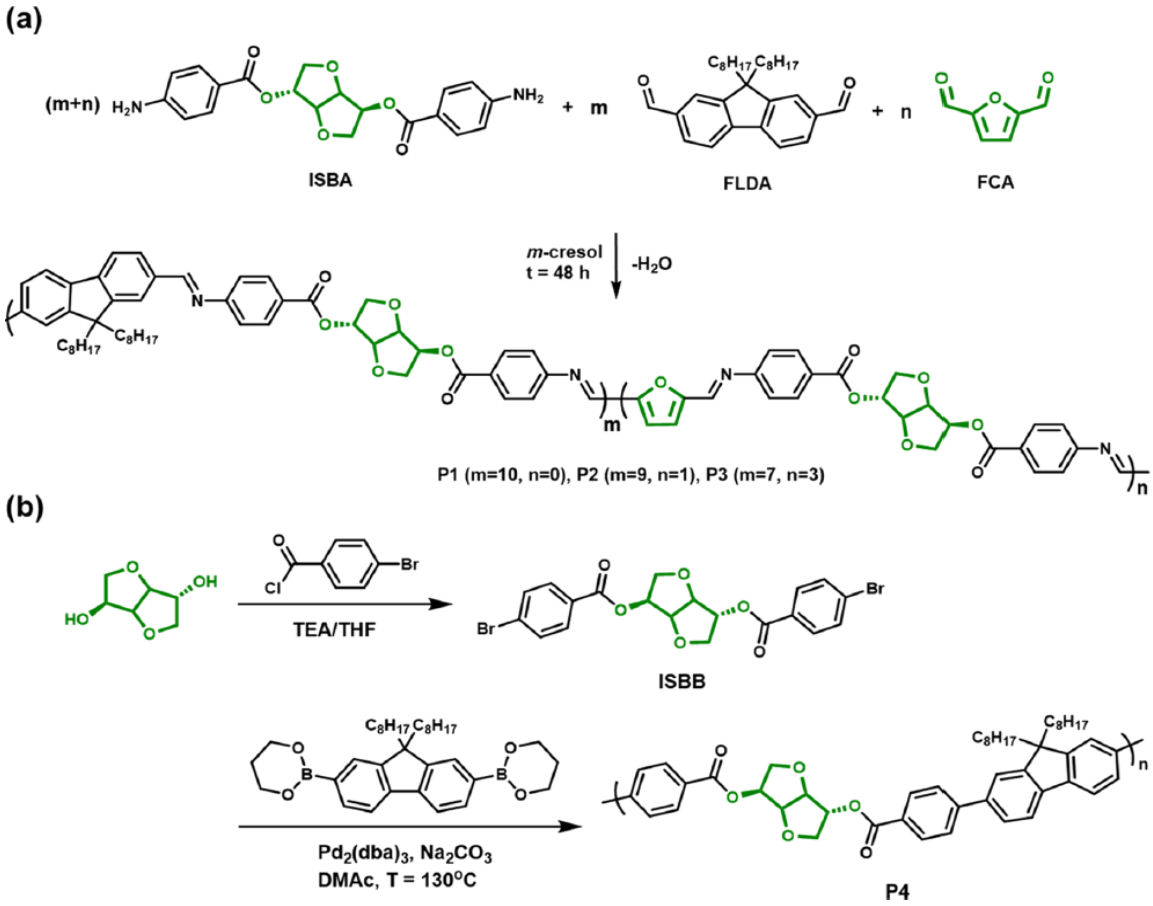

Scheme 5. Synthesis of (a) poly(azomethine)s (**P1** – **P3**) with various molar ratios of FLDA (m) and FCA (n) and (b) Photoactive polymer (**P4**) without imine linkages. Reprinted with permission from ACS Sustain. Chem. Eng. 10 (2022) 5268. [54] Copyright 2022 American Chemical Society.

Polymers **P1**–**P3** were observed to possess smaller band gaps (2.83−2.86 eV) than **P4** (3.11 eV) due to longer π-conjugation lengths and structural coplanarity due to the imine linkages. The imine-containing polymers were also found to be more thermally robust, showing higher T_g values. All the polymers proved effective in exhibiting photowriting or electrical erasing characteristics when employed as chargeable electrets in OFET-based memory devices using pentacene as the semiconductor. These OFET memories incorporating **P1**−**P4** as electrets exhibited memory windows of 17−25 V and memory ratios as high as 2.1×10^4 with

photowriting-electrical-erasing characteristics. Subsequently, the authors fabricated a flexible device using a biobased polyimide as the substrate and the dielectric layer. The flexible photomemory presented impressive long-term stability and endurance, i.e., a memory ratio of 1.3×10^3 maintained for 10^4 s in the retention test and 1.3×10^3 over 50 WRER cycles. More impressively, these memory properties were preserved even after 1000 cycles of bending under a 5 mm bending radius. In terms of degradability, the presence of hydrolytically labile imine and ester linkages enabled the polymers to degrade into smaller biosegments under acidic conditions within a single week. Taken together, the combined physicochemical properties of these poly(azomethine)s make them very promising as potentially sustainable next-generation green electronics.

In the following year, the Chen group continued their sustainability-focused work on photonic memory devices with flexible bio-derived electrets (Fig. 12). This time, they reported degradable biobased polylactic acid (PLA) electrets with photoactive hemin or protoporphyrin IX (PPIX) embedded within the polymer. [55] The inspiration behind this was to offer a greener alternative to floating-gate electrets made from heavy metal-based quantum dots. PLA itself can be synthesized via microbial fermentation or through ring-opening polymerization of lactide. In essence, this all-organic composite system leveraged the electret properties of the insulating PLA and the photophysical properties of naturally-occurring porphyrins for memory applications.

The PPIX/PLA-based device was observed to have a high memory ratio of 2.5×10^7 upon light removal for 10^4 s, which was superior to that of hemin/PLA-based device (1.8×10^4). The high memory ratio and persistence of the PPIX/PLA system could be attributed to its relaxation dynamics as well as its core structure that provided extra sites for charge consolidation. Charge storage in hemin, on the other hand, was challenging due to self-charge transfer during relaxation and the reduced number of trapping sites due to chelated Fe(III) ions.

The discreteness of charge-trapping sites significantly affected the memory ratio. Furthermore, the flexible photomemory also utilized a biobased polyimide as both the substrate and dielectric layer, and the device employing the PPIX/PLA-based electret was able to maintain a high memory ratio of 8.9×10^5 after 10^4 s in a retention test. In regards to device durability, the PPIX/PLA-based electret retained its memory even after 1000 cycles of bending with a 5 mm bending radius. Overall, these studies further highlighted the potential of using polymeric bioelectrets for sustainable photonic memories.

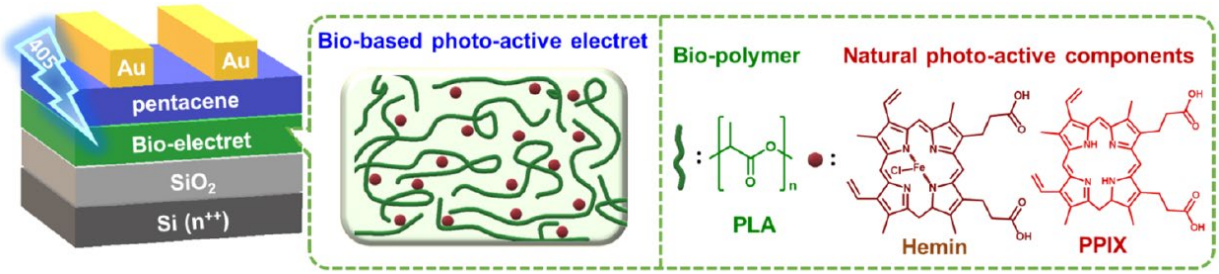

Fig. 12. Schematic of the photomemory device employing biobased photoactive electrets. Adapted with permission from ACS Appl. Mater. Interfaces. 15 (2023) 33829 [55]. Copyright 2023 American Chemical Society.

Aside from degradable biobased polymer electrets aimed at greater sustainability, researchers have also leveraged advances from other subfields in organic electronics and applied them to developing advanced memory technologies. For instance, the development of novel AIE luminogens (AIEgens) has been a hot topic in its own right over the past decade. Subsequently, Liou and Liu (coauthor of this review) showed that AIE-fluorescent electrets were also useful for photomemory storage applications [58]. More recently, Liou and coworkers [59] reported high-performance AIE-active poly(ether sulfone)s as effective polymeric electrets in energy-saving photonic transistor memories. Specifically, their work featured AIE-active polymer electrets composed of a partially π-conjugated triphenylamine (TPA)/poly(ether sulfone) (PES) backbone functionalized with pendent AIE-active groups,

i.e., α-cyanostilbene (CNBr) and tetraphenylethylene (TPE). The two polymers (CNBr-PES and TPE-PES) were synthesized via SNAr-based nucleophilic polycondensation between the AIEgen-bearing TPA comonomer and the sulfone-containing difluoride (Scheme 6).

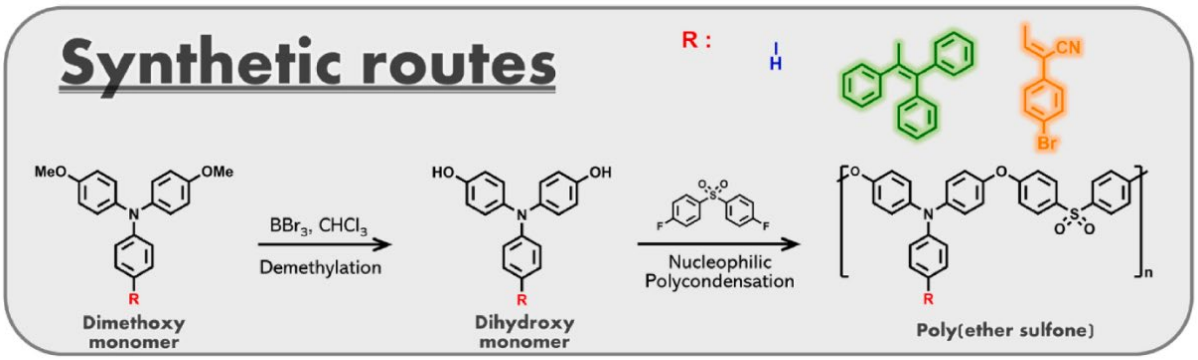

Scheme 6. Synthesis of two AIE-active polymer electrets by Liou and coworkers. Adapted from ref. [59], with permission from Elsevier.

For photoprogramming purposes, the memory devices fabricated with TPE-PES and CNBr-PES polymers showed memory windows of 10 V and 50 V, respectively. The unique structural moieties within the polymer electrets played specialized roles in terms of function and performance. The orthogonally connected TPA donors and TPE/CNBr acceptors, with their mutually non-overlapping HOMOs and LUMOs, served as the AIE handles. The ether linkages between the TPA and PES moieties disrupted π-conjugation along the polymer backbone, which helped promote memory stability and durability. Lastly, the aromatic sulfones provided an ideal environment for pentacene growth and promoted large semiconducting domains with fewer crystal boundaries. The resulting PES-based photonic devices exhibited nonvolatile photonic memory behavior, excellent retention (14 days), and low working voltages (V_{GS} = 0V; V_{DS} = –5V). All in all, this study demonstrated how the properties of PES and AIEgens could be combined in a single homopolymer electret to create energy-saving photomemory devices with excellent performance.

4. Conclusions and perspectives

With the increasing interest in organic memory, photomemory, and artificial synaptic technologies over the past decade, researchers have been constantly seeking new ways to improve device performance. Aside from the organic semiconductors, the other key organic component of memory devices are the polymer electrets that serve the role of charge-trapping and storage. As evidenced by the wealth of diverse polymeric systems that have been reported in the last 4-5 years (i.e., those discussed in this review), research activity in this area is expected to continue unabated. The ease and modularity of the synthesis of pendent sidechain polymers and π-conjugated polymers suggest that we will likely continue to see future electret systems from these categories. Researchers may also adopt a 'mix-and-match' approach to create novel structures and molecular assemblies from just these two categories of polymers alone. Moving forward, one can also anticipate the advent of many more biobased and biodegradable polymer systems similar to those covered in the final section. This is in line with the increasing focus on sustainability and circularity within scientific circles, driven by the global crisis concerning pollution and dwindling nonrenewable resources. Finally, given the trend of using artificial intelligence and machine learning in materials research, one can also expect that future polymer electrets with customizable properties will be increasingly designed by a combination of chemical intuition, human ingenuity, and high-performance computing.

Declaration of competing interest

The authors declare that they have no known competing interests or personal relationships that could have appeared to influence the work reported in this paper.

Data availability

No data was used for the research described in the article.

Acknowledgments

J.M.W.C. is supported by the Agency for Science, Technology and Research, under A*STAR Project No. C210812024 (2021 A*STAR CDF) and the 2022 SERC Central Research Fund UIBR. C.-L.L. acknowledges the financial support from 2030 Cross-Generation Young Scholars Program by the National Science and Technology Council (NSTC) in Taiwan under grant 113-2628-E-002-009 and Advanced Research Center for Green Materials Science and Technology from The Featured Area Research Center Program within the framework of the Higher Education Sprout Project by the Ministry of Education (113L9006).

References

[1] C. C. Shih, Y. C. Chiang, H. C. Hsieh, Y. C. Lin, W. C. Chen, Multilevel Photonic Transistor Memory Devices Using Conjugated/Insulated Polymer Blend Electrets., ACS Appl. Mater. Interfaces, 11 (2019) 42429.

[2] Z. Y. Wei, S. P. Prakoso, Y. T. Li, Y. C. Chiu, Tunneling-Effect-Boosted Interfacial Charge Trapping toward Photo-Organic Transistor Memory., Adv. Electron. Mater., 8 (2022) 2101349.

[3] C. H. Chen, Y. Wang, H. Tatsumi, T. Michinobu, S. W. Chang, Y. C. Chiu, G. S. Liou, Novel Photoinduced Recovery of OFET Memories Based on Ambipolar Polymer Electret for Photorecorder Application., Adv. Funct. Mater., 29 (2019) 1902991.

[4] R. Mitobe, Y. Sasaki, W. Tang, Q. Zhou, X. Lyu, K. Ohshiro, M. Kamiko, T. Minami, Multi-Oxyanion Detection by an Organic Field-Effect Transistor with Pattern Recognition

Techniques and Its Application to Quantitative Phosphate Sensing in Human Blood Serum., ACS Appl. Mater. Interfaces, 14 (2022) 22903.

[5] C.-C. Hung, Y.-C. Chiang, Y.-C. Lin, Y.-C. Chiu, W.-C. Chen, Conception of a Smart Artificial Retina Based on a Dual-Mode Organic Sensing Inverter, Adv. Sci., 8 (2021) 2100742

[6] Z. Shao, T. Jiang, X. Zhang, X. Zhang, X. Wu, F. Xia, S. Xiong, S. T. Lee, J. Jie, Memory phototransistors based on exponential-association photoelectric conversion law, Nat. Commun., 10 (2019) 1294.

[7] T. Ahmed, M. Tahir, M. X. Low, Y. Ren, S. A. Tawfik, E. L. H. Mayes, S. Kuriakose, S. Nawaz, M. J. S. Spencer, H. Chen, M. Bhaskaran, S. Sriram, S. Walia, Fully Light-Controlled Memory and Neuromorphic Computation in Layered Black Phosphorus., Adv. Mater., 33 (2021) 2004207.

[8] M. M. Mburu, K. T. Lu, N. L. Prine, A. N. Au-Duong, W. H. Chiang, X. Gu, Y. C. Chiu, Conjugated Polymer-Wrapped Single-Wall Carbon Nanotubes for High-Mobility Photonic/Electrical Fully Modulated Synaptic Transistor, Adv. Mater. Technol., 7 (2022) 2101506.

[9] Z. He, J. Han, X. Du, L. Cao, J. Wang, C. Zheng, H. Lin, S. Tao, Photomemory and Pulse Monitoring Featured Solution-Processed Near-Infrared Graphene/Organic Phototransistor with Detectivity of 2.4×10^{13} Jones, Adv. Funct. Mater., 31 (2021) 2103988.

[10] Z. Zhu, Y. Guo, Y. Liu., Application of organic field-effect transistors in memory, Mater. Chem. Front., 4 (2020) 2845

[11] C.-C. Shih, W. Y. Lee, W. C. Chen, Nanostructured materials for non-volatile organic transistor memory applications, Mater. Horiz., 3 (2016) 294.

[12] Z. Zhu, Y. Guo, Y. Liu, Application of organic field-effect transistors in memory., Mater. Chem. Front., 4 (2020) 2845.

[13] S. P. Prakoso, M.-N. Y.-C. Chiu, A brief review on device operations and working mechanisms of organic transistor photomemories, J. Mater. Chem. C, 10 (2022) 13462.

[14] K.-J. Baeg, Y.-Y. Noh, J. Ghim, B. Lim, D.-Y. Kim, Polarity Effects of Polymer Gate Electrets on Non-Volatile Organic Field-Effect Transistor Memory., Adv. Funct. Mater. 18 (2008) 3678.

[15] S. Lee, S. Kim, H. Yoo, Contribution of Polymers to Electronic Memory Devices and Applications, Polymers, 13 (2021) 3774.

[16] T.-W. Chang, Y.-S. Li, N. Matsuhisa, C.-C. Shih, Emerging polymer electrets for transistor-structured memory devices and artificial synapses, J. Mater. Chem. C., 10 (2022) 13372.

[17] Y. Yu, Q. Ma, H. Ling, W. Li, R. Ju, L. Bian, N. Shi, Y. Qian, M. Yi, L. Xie, W. Huang, Small-Molecule-Based Organic Field-Effect Transistor for Nonvolatile Memory and Artificial Synapse, Adv. Funct. Mater., 29 (2019) 1904602.

[18] Y. Ni, Y. Wang, W. Xu, Recent Process of Flexible Transistor-Structured Memory, Small, 17 (2021) 1905332.

[19] Y.-H. Chou, H.-C. Chang, C.-L. Liu, W.-C. Chen, Polymeric charge storage electrets for non-volatile organic field effect transistor memory devices, Polym. Chem., 6 (2015) 341.

[20] J. M. Lee, I. T. Cho, J. H. Lee, H. I. Kwon, Bias-stress-induced stretched-exponential time dependence of threshold voltage shift in InGaZnO thin film transistors, Appl. Phys. Lett., 93 (2008) 093504.

[21] H. F. Haneef, A. M. Zeidell, O. D. Jurchescu, Charge carrier traps in organic semiconductors: a review on the underlying physics and impact on electronic devices, J. Mater. Chem. C, 8 (2020) 759–787.

[22] Y.-C. Lin, W.-C. Yang, Y.-C. Chiang, W.-C. Chen, Recent advances in organic phototransistors: nonvolatile memory, artificial synapses, and photodetectors, Small Sci., 2 (2022) 2100109.

[23] X. Wu, D. Dai, W. Huang, S. Feng, W. Huang, High-k polymer dielectrics with different cross-linked networks for nonvolatile transistor memory device. Org. Electron., 96 (2021) 106222.

[24] P. Evan, K. Tejaswini, S. Q. Zhang, H. E. Katz, D. H. Reich, Effects of trifluoromethyl substituents on interfacial and bulk polarization of polystyrene gate dielectrics, Appl. Phys. Lett., 114 (2019) 023301.

[25] G. Zhang, Y. J. Lee, P. Gautam, C. C. Lin, C.-L. Liu, J. M. W. Chan, Pentafluorosulfanylated polymers as electrets in nonvolatile organic field-effect transistor memory devices, J. Mater. Chem. C, 7 (2019) 7865–7871.

[26] J. M. W. Chan, Pentafluorosulfanyl group: an emerging tool in optoelectronic materials, J. Mater. Chem. C, 7 (2019), 12822–12834.

[27] Y. Zhu, Y. Fan, S. Li, P. Wei, D. Li, B. Liu, D. Cui, Z. Zhang, G. Li, Y. Nie, G. Lu, Soluble poly(4-fluorostyrene): a high-performance dielectric electret for organic transistors and memories, Mater. Horizons, 7 (2020) 1861.

[28] T. Xu, Y. Liu, Y. Bu, S. Shu, S. Fan, M. Cao, T. Liu, J. Zou, J. Su, Newly Synthesized High-k Polymeric Dielectrics with Cyclic Carbonate Functionality for Highly Stability Organic Field-Effect Transistor Applications, Adv. Electron. Mater., 9 (2023) 2200984.

[29] Y.-H. Weng, Y. C. Lin, J. C. Ho, W. C. Yang, B. H. Lin, C.-L. Liu, W. C. Chen, High-Performance Phototransistor Memory with an Ultrahigh Memory Ratio Conferred Using Hydrogen-Bonded Supramolecular Electrets, ACS Appl. Mater. Interfaces, 15 (2023) 19258.

[30] L. Wang, C. Zheng, J. Fu, J. Hua, J. Chen, J. Gao, H. Ling, L. Xie, W. Huang, Influence of Molecular Weight of Polymer Electret on the Synaptic Organic Field-Effect Transistor Performance, Advanced Electronic Materials 2022, 8 (9), 2200155.

[31] M. Yi, M. Xie, Y. Shao, W. Li, H. Ling, L. Xie, T. Yang, Q. Fan, J. Zhu, W. Huang, Light programmable/erasable organic field-effect transistor ambipolar memory devices based on the pentacene/PVK active layer, J. Mater. Chem. C, 3 (2015) 5220.

[32] M.-N. Chen, S.-W. Chang, S. P. Prakoso, Y.-T. Li, K.-L. Chen, Y.-C. Chiu, Unveiling the Photoinduced Recovery Mystery in Conjugated Polymer-Based Transistor Memory, ACS Appl. Mater. Interfaces, 13 (2021) 44656.

[33] C.-Y. Ke, M.-N. Chen, Y.-C. Chiu, G.-S. Liou, Luminescence Behavior and Acceptor Effects of Ambipolar Polymeric Electret on Photorecoverable Organic Field-Effect Transistor Memory, Adv. Electron. Mater., 7 (2021) 2001076.

[34] W. Wu, H. Zhang, Y. Wang, S. Ye, Y. Guo, C. Di, G. Yu, D. Zhu, Y. Liu, High-Performance Organic Transistor Memory Elements with Steep Flanks of Hysteresis, Adv. Funct. Mater., 18 (2008) 2593.

[35] X. Wu, Y. Chu, R. Liu, H. E. Katz, J. Huang, Pursuing Polymer Dielectric Interfacial Effect in Organic Transistors for Photosensing Performance Optimization, Adv. Sci., 4 (2017) 1700442.

[36] Y. Li, Q. Feng, H. Ling, Y. Chang, Z. Liu, H. Liu, L. Xie, C. Yin, M. Yi, W. Huang, Bulky side chain effect of poly(N-vinylcarbazole)-based stacked polymer electrets on device performance parameters of transistor memories, J. Polym. Sci., Part A: Polym. Chem., 55 (2017) 3554.

[37] J. Lin, W. Li, Z. Yu, M. Yi, H. Ling, L. Xie, S. Li, W. Huang, π-Conjugation-interrupted hyperbranched polymer electrets for organic nonvolatile transistor memory devices, J. Mater. Chem. C, 2 (2014) 3738.

[38] Y.-C. Chiu, I. Otsuka, S. Halila, R. Borsali, W.-C. Chen, High-Performance Nonvolatile Transistor Memories of Pentacence Using the Green Electrets of Sugar-based Block Copolymers and Their Supramolecules, Adv. Funct. Mater., 24 (2014) 4240.

[39] H. Ling, J. Lin, M. Yi, B. Liu, W. Li, Z. Lin, L. Xie, Y. Bao, F. Guo, W. Huang, Synergistic Effects of Self-Doped Nanostructures as Charge Trapping Elements in Organic Field Effect Transistor Memory, ACS Appl. Mater. Interfaces, 8 (2016) 18969.

[40] S. H. Kim, S. Nam, J. Jang, K. Hong, C. Yang, D. S. Chung, C. E. Park, W.-S. Choi, Hysteresis behaviour of low-voltage organic field-effect transistors employing high dielectric constant polymer gate dielectrics, J. Appl. Phys., 43 (2010) 465102.

[41] L.-C. Hsu, T. Isono, Y.-C. Lin, S. Kobayashi, Y.-C. Chiang, D.-H. Jiang, C.-C. Hung, E. Ercan, W.-C. Yang, H.-C. Hsieh, K. Tajima, T. Satoh, W.-C. Chen, Stretchable OFET Memories: Tuning the Morphology and the Charge-Trapping Ability of Conjugated Block Copolymers through Soft Segment Branching, ACS Appl. Mater. Interfaces, 13 (2021) 2932.

[42] H. Ling, W. Li, H. Li, M. Yi, L. Xie, L. Wang, Y. Ma, Y. Bao, F. Guo, W. Huang, Effect of thickness of polymer electret on charge trapping properties of pentacene-based nonvolatile field-effect transistor memory, Org. Electron., 43 (2017) 222.

[43] T. Michinobu, H. Osako; C. Seo, K. Murata, T. Mori, K. Shigehara, Multicolor emission and thin film transistor properties of 1,8-diethynylcarbazole-based conjugated copolymers. Polymer, 52 (2011) 5756.

[44] C.-H. Chen, Y. Wang, T. Michinobu, S. W. Chang, Y. C. Chiu, C. Y. Ke, G. S. Liou, Donor-Acceptor Effect of Carbazole-Based Conjugated Polymer Electrets on Photoresponsive Flash Organic Field-Effect Transistor Memories, ACS Appl. Mater. Interfaces, 12 (2020) 6144.

[45] W. C. Yang, E. Ercan, Y. C. Lin, W. C. Chen, Y. Watanabe, K. Nakabayashi, B. H. Lin, C. T. Lo, H. Mori, W. C. Chen, High-Performance Organic Photosynaptic Transistors Using Donor−Acceptor Type and Crosslinked Core−Shell Nanoparticles as a Floating Gate Electret, Adv. Opt. Mater., 11 (2022) 2202110.

[46] Y. T. Yang, Y. S. Wu, W. He, H. C. Tien, W. C. Yang, T. Michinobu, W. C. Chen, W. Y. Lee, C. C. Chueh, Tuning Ambipolarity of the Conjugated Polymer Channel Layers of Floating-Gate Free Transistors: From Volatile Memories to Artificial Synapses, Adv. Sci., 9 (2022) e2203025.

[47] C. Y. Ke, M. N. Chen, M. H. Chen, Y. T. Li, Y. C. Chiu, G. S. Liou, Novel Authentic and Ultrafast Organic Photorecorders Enhanced by AIE-Active Polymer Electrets via Interlayer Charge Recombination, Adv. Func. Mater., 31 (2021) 210128.

[48] Y.-C. Chen, Y.-C. Lin, H.-C. Hsieh, L.-C. Hsu, W.-C. Yang, T. Isono, T. Satoh, W.-C. Chen, Improving the performance of photonic transistor memory devices using conjugated block copolymers as a floating gate, J. Mater. Chem. C, 9 (2021) 1259.

[49] L.-C. Hsu, T. Isono, Y. C. Lin, S. Kobayashi, Y. C. Chiang, D. H. Jiang, C. C. Hung, E. Ercan, W. C. Yang, H. C. Hsieh, K. Tajima, T. Satoh, W. C. Chen, Stretchable OFET Memories: Tuning the Morphology and the Charge-Trapping Ability of Conjugated Block Copolymers through Soft Segment Branching, ACS Appl. Mater. Interfaces, 13 (2021) 2932.

[50] C. F. Lin, Y. C. Lin, W. C. Yang, L. C. Hsu, E. Ercan, C. C. Hung, Y. Y. Yu, W. C. Chen, Multiband Photoresponding Field-Effect Transistor Memory Using Conjugated Block Copolymers with Pendent Isoindigo Coils as a Polymer Electret, Adv. Electron. Mater., 7 (2021) 2100655.

[51] E. Ercan, L.-C. Hsu, Y.-C. Lin, B.-H. Lin, W.-C. Chen, Multistimuli-Responsive Plasticity Transitions of a Phototransistor Conferred by Using Thermoresponsive Polyfluorene Block Copolymers, ACS Appl. Polym. Mater., 5 (2023) 463.

[52] Y. C. Chiu, Y. Chen, C. C. Kuo, S. H. Tung, T. Kakuchi, W. C. Chen, Synthesis, morphology, and sensory applications of multifunctional rod−coil−coil triblock copolymers and their electrospun nanofibers, ACS Appl. Mater. Interfaces, 4 (2012) 3387.

[53] Y.-F. Yang, Y.-C. Lin, E. Ercan, Y.-C. Chiang, B.-H. Lin, W.-C. Chen, Improving the Photoresponse of Transistor Memory Using Self-Assembled Nanostructured Block Copolymers as a Photoactive Electret, Macromolecules, 55 (2022) 8262.

[54] C.-K. Chen, Y.-C. Lin, J.-C. Ho, W.-C. Yang, W.-C. Chen, Biomass-Derived Degradable Poly(azomethine)s for Flexible Bistable Photonic Transistor Memories, ACS Sustain. Chem. Eng. 10 (2022) 5268.

[55] C. K. Chen, J. C. Ho, C. C. Hung, W. C. Chen, T. Satoh, W. C. Chen, Sustained Flexible Photonic Transistor Memories Based on Fully Natural Floating Gate Electrets, ACS Appl. Mater. Interfaces, 15 (2023) 33829.

[56] T. Mulia, M. Mumtaz, E. Ercan, W.-C. Yang, C.-F. Lin, Y.-C. Lin, R. Borsali, W.-C. Chen, Exploring the Charge-Trapping Behavior of Self-Assembled Sugar-based Block Copolymers with a Pendent Design in Photoassisted Memory, ACS Appl. Polym. Mater., 5 (2023) 3898.

[57] J.-H. Yeh, S. P. Prakoso, L. L. Santoso, S.-J. Chen, B. Chiang, J.-C. Cheng, R.-N. Zhang, Y.-C. Chiu, A sustainable biomass-based electret for face mask and non-volatile transistor memory, Organic Electron., 124 (2024) 106944.

[58] T.-Y. Huang, C.-H. Chen, C.-C. Lin, Y.-J. Lee, C.-L. Liu, G.-S. Liou, UV-sensing organic phototransistor memory devices with a doped organic polymer electret composed of triphenylamine-based aggregation-induced emission luminogens, J. Mater. Chem. C, 7 (2019) 11014.

[59] C.-Y. Ke, M.-H. Chen, G.-S. Liou, High-performance aggregation-induced emission active poly(ether sulfone)s as polymeric electret for energy-saving genuine photonic transistor memory, Chem. Eng. J. 457 (2023) 141209.